Electronic Supplementary Information (ESI)

Microporous polyurethane material for size selective heterogeneous catalysis of the Knoevenagel reaction

Sandeep Kumar Dey,‡ Nader de Sousa Amadeu and Christoph Janiak*

Institut für Anorganische Chemie und Strukturchemie, Heinrich-Heine-Universität Düsseldorf, 40204 Düsseldorf, Germany. E-mail: janiak@uni-duesseldorf.de

Fax: +49-211-81-12287; Tel: +49-211-81-12286

‡ Research fellow funded by Alexander von Humboldt Foundation, D-53173 Bonn, Germany.

Table of contents:

1. Materials and methods

All chemicals were purchased from commercial suppliers (Sigma-Aldrich, Acros Organics, and Alfa Aesar chemical company) and used without further purification. Infrared (IR) spectra were recorded on a Bruker FT-IR Tensor 37 Spectrometer in the 4000-400 cm^{-1} region with 2 cm^{-1} resolution as KBr disks. ^{1}H and ^{13}C spectra were recorded on a Bruker 300 MHz instrument. ^{1}H and ^{13}C NMR chemical shifts are given in ppm relative to $SiMe_4$ (δ = 0.0 ppm) with calibration against the (residual protonated) $CDCl_3$ signal 7.26 (^{1}H) and 77.0 (^{13}C). Elemental (CHNS) analyses were carried out with a Perkin-Elmer 2400 Series-2 elemental analyser. Powder X-ray diffraction (PXRD) data were collected on a Bruker D2 Phaser diffractometer using a flat sample holder and Cu $K\alpha_1/\alpha_2$ radiation with λ = 1.5418 Å at 30 kV covering 2θ angles 5-70° over a time of 8 h. Thermogravimetric analyses (TGA) were carried out at a ramp rate of 2°C/min in a N_2 flow with a Netzsch Thermo-Microbalance Apparatus TG 209 F3 Tarsus. Energy dispersive X-ray spectrometric (EDX) measurements were carried out on a JEOL scanning electron microscope JSM-6510 with tungsten (W) cathode and an EDX unit. The samples were coated with Au for 20 s at 30 mA by using a JEOL JFC-1200 sputter coater (JSM-6510). Nitrogen sorption isotherms at 77 K were obtained using a NOVA-4000e instrument within a partial pressure range of 10^{-6}–1.0. DFT calculations for the pore size distribution curves were carried out using the native ASiQWin 1.2 software employing the N_2 at 77 K on carbon, slit pore, NLDFT equilibrium model. CO_2 sorption were measured using a Micromeritics ASAP 2020 automatic gas sorption analyzer equipped with oil-free vacuum pumps (ultimate vacuum $<10^{-8}$ mbar) and valves, which guaranteed contamination free measurements. Potentiometric titrations were performed using a Metrohm 848 Titrino automatic titrator for volumetric titrations.

2. Solvothermal synthesis of microporous polyurethane (MPU)

Most of the other porous polyurethanes described in literature (for soft tissue engineering applications) are flexible in nature, synthesized by combining polyethylene glycol (or polypropylene glycol) or polycaprolactone diol with various diisocyanates in the presence of porogens (references 11 and 12 in the main text). These other porous polyurethanes do not have a clearly reported microporosity, that is, they do not give a clear indication of pore diameters below 2 nm (ref. 11 and 12 in main text).

Following the chemistry of covalent organic frameworks (COFs), we intend to develop a new porous and rigid polyurethane framework for gas sorption application and heterogeneous catalysis. The reaction between phloroglucinol (2 mmol) and 1,4-phenylenediisocyanate (3 mmol) in DMSO was carried out under unprecedented solvothermal conditions. Solvothermal synthesis conditions have not been previously employed for the synthesis of other porous polyurethanes to the best of our knowledge. It was our aim to control the crystallinity of the material, since crystalline materials have homogeneous pore distribution.

The microporous polyurethane (MPU) was synthesized by the condensation of phloroglucinol (252 mg, 2 mmol) and 1,4-phenylenediisocyanate (480 mg, 3 mmol) in dimethyl sulfoxide (20 mL) in a Teflon-lined stainless steel autoclave heated at 150 °C for 72 h (Scheme 1), followed by slow cooling over a period of 16 h. A dark brown solid thus obtained was collected in a beaker, to which 100 mL of acetone was added and stirred for an hour followed by filtration. The product was further washed with acetone for a couple of times, each for a period of ~ 2 h under stirring at room temperature. The product was then washed with 50 mL of tetrahydrofuran (THF) under stirring at room

temperature and this was repeated for another couple of times, each for a period of ~ 2 h. The product was then repeatedly washed with methanol under stirring at room temperature (~ 5 times, each time for ~ 10-12 h). Finally, the product was collected by filtration and was dried at 150 °C under vacuum for 48 h to yield activated **MPU** as dark brown powder (560 mg, yield 76%).

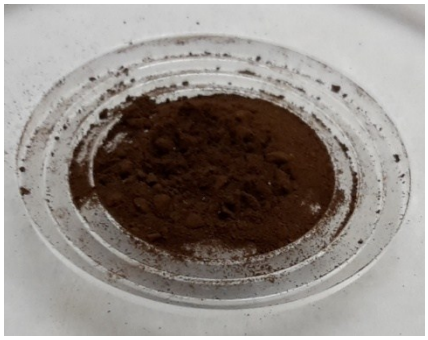

Fig. S1 Camera image of the activated MPU.

3. General procedures of heterogeneous catalysis by the activated MPU

Knoevenagel reaction: The Knoevenagel reaction between an aromatic aldehyde and an active methylene compound (malononitrile/methylcyanoacetate) using the activated MPU catalyst was carried out in a magnetically stirred round bottom flask at 50 °C in tetrahydrofuran (THF). In a typical reaction, a mixture of benzaldehyde (106 mg, 1.0 mmol) and malononitrile (72 mg, 1.1 mol) was dissolved in 10 ml of THF in a round bottom flask and 5 mol% (18 mg) of the MPU catalyst was added into it. The heterogeneous solution mixture was then stirred at 50 °C for 14 h. The MPU catalyst was separated from the reaction mixture by simple filtration, and the filtrate was concentrated under reduced pressure and dried under vacuum. The yield was calculated from ^{1}H NMR analysis of the crude product, measuring the integral values of the product and the unreacted aldehyde. The crude product was purified by recrystallization from methanol/ethanol to afford pure compounds.

Henry (Nitroaldol) reaction: The Henry reaction between an aromatic aldehyde and nitromethane using the activated MPU catalyst was carried out at 50 °C in methanol. In a typical reaction, a mixture of nitrobenzaldehyde (151 mg, 1.0 mmol) and nitromethane (610 mg, 10 mmol) was dissolved in 10 ml of methanol in a round bottom flask and 5 mol% (18 mg) of the MPU catalyst was added into it. The heterogeneous solution was then stirred at 50 °C for 10 h. The MPU catalyst was separated from the reaction mixture by simple filtration, and the filtrate was concentrated under reduced pressure and dried under vacuum. The yield was calculated from ^{1}H NMR analysis of the crude product, measuring the integral values of the product and the unreacted aldehyde.

Catalyst recyclability

In order to examine the catalyst recyclability and stability in the Knoevenagel reaction, the MPU has been recovered from the heterogeneous reaction mixture by simple filtration and washed repeatedly with acetone under stirring at room temperature (~ 3 times, each time for ~ 2 h). The product was then repeatedly washed with methanol under stirring at room temperature (~ 5 times, each time for ~ 10-12 h), till the filtrate is clear and free from any yellow coloration. Finally, the

product was collected by filtration and was dried at 150 °C under vacuum for 48 h to yield activated **MPU** as dark brown powder.

Table S1 Nitrogen sorption (77 K) obtained BET and Langmuir surface areas of the activated MPU (two batches prepared) and recycled MPU after first and second catalytic run.

Samples	S_{BET} (m^2/g)	S_{Lang} (m^2/g)
MPU-Batch-1	308	502
MPU-Batch-2	316	514
MPU-Recycled1	286	489
MPU-Recycled2	280	481

Table S2 CHNS analysis of the activated MPU (two batches prepared), and recycled MPU after first and second catalysis cycle.

Samples	Calculated				Experimental				
	C%	H%	N%	S%	C%	H%	N%	S%	DMSO%
MPU-Batch1	58.86	3.57	11.44	—	61.55	4.38	11.19	2.05	6.62
MPU-Batch2	58.86	3.57	11.44	—	61.91	4.64	11.42	2.24	7.25
MPU-Recycled1	58.86	3.57	11.44	—	60.71	4.63	11.34	2.18	7.00
MPU-Recycled2	58.86	3.57	11.44	—	60.60	4.19	11.25	2.07	6.64

4. Characterization of the microporous polyurethane (MPU) material.

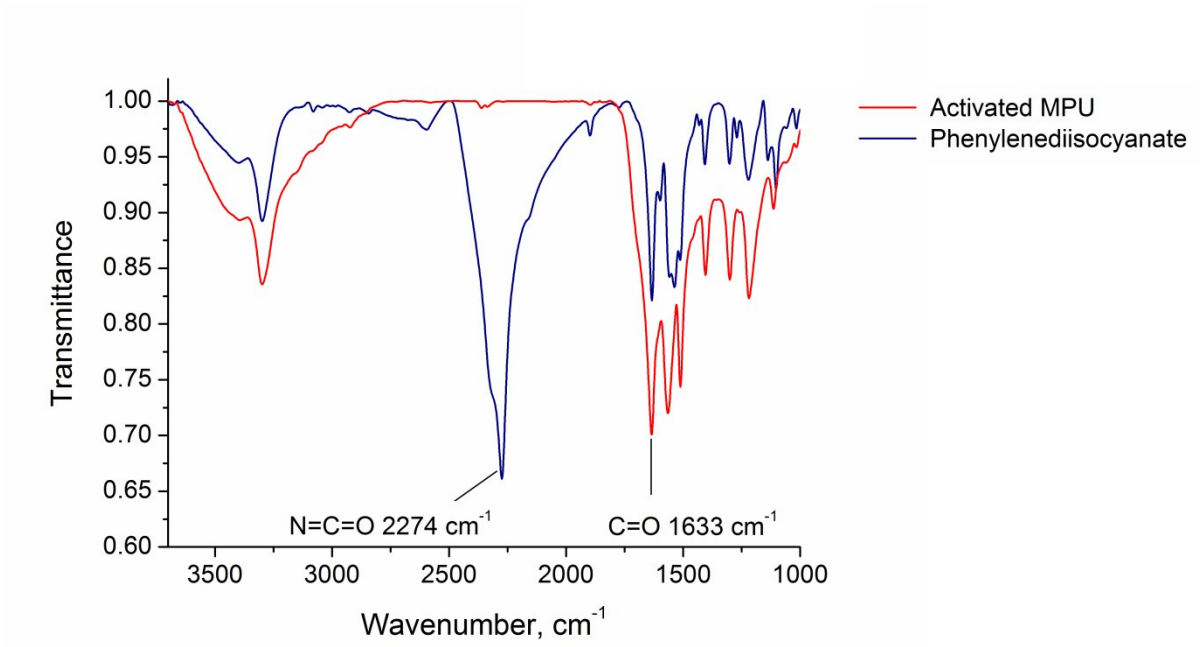

Fig. S2 Comparison of the FT-IR spectra of 1,4-phenylenediisocyanate with the activated MPU.

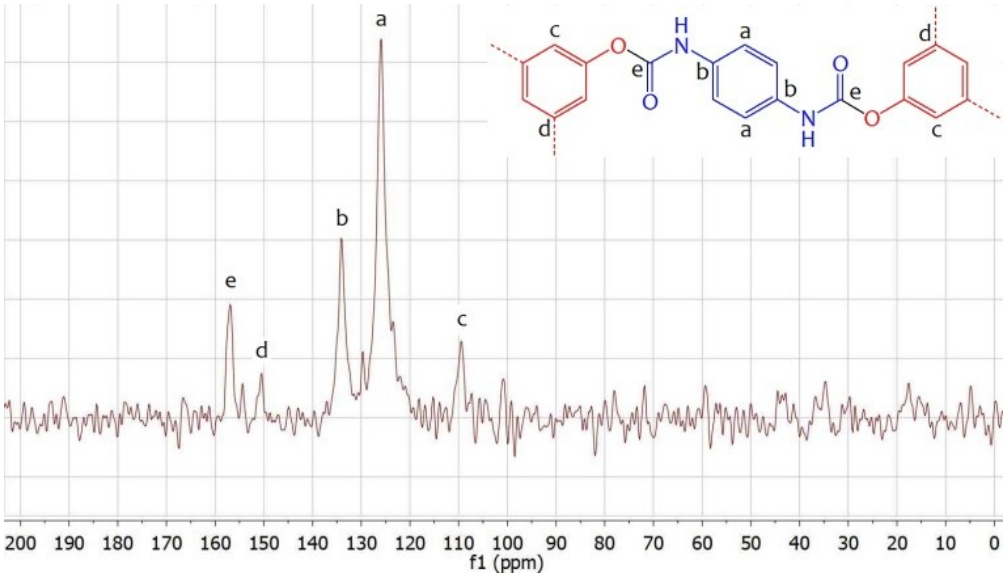

Fig. S3 Solid-state ^{13}C NMR spectrum of the activated MPU material.

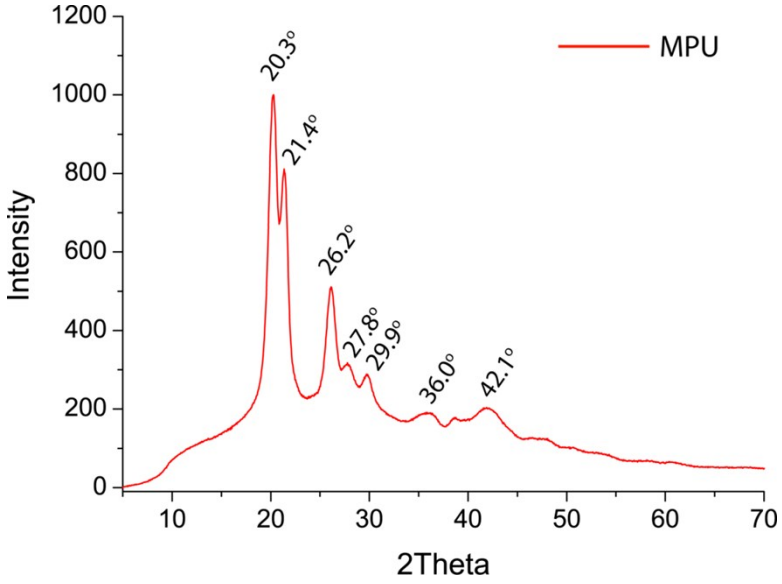

Fig. S4 Powder X-ray diffraction (PXRD) pattern of the activated MPU.

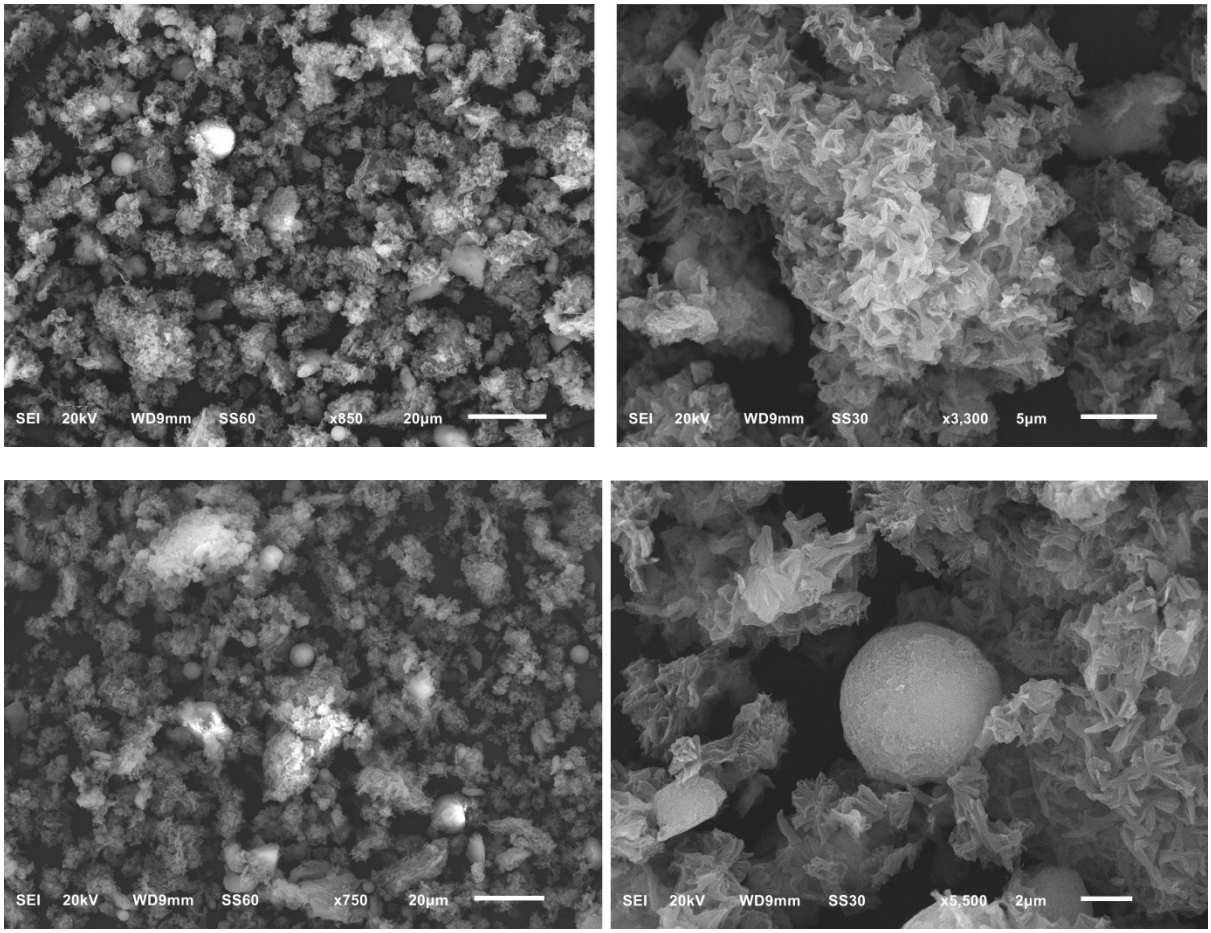

Fig. S5 Scanning electron microscope (SEM) images of the activated MPU.

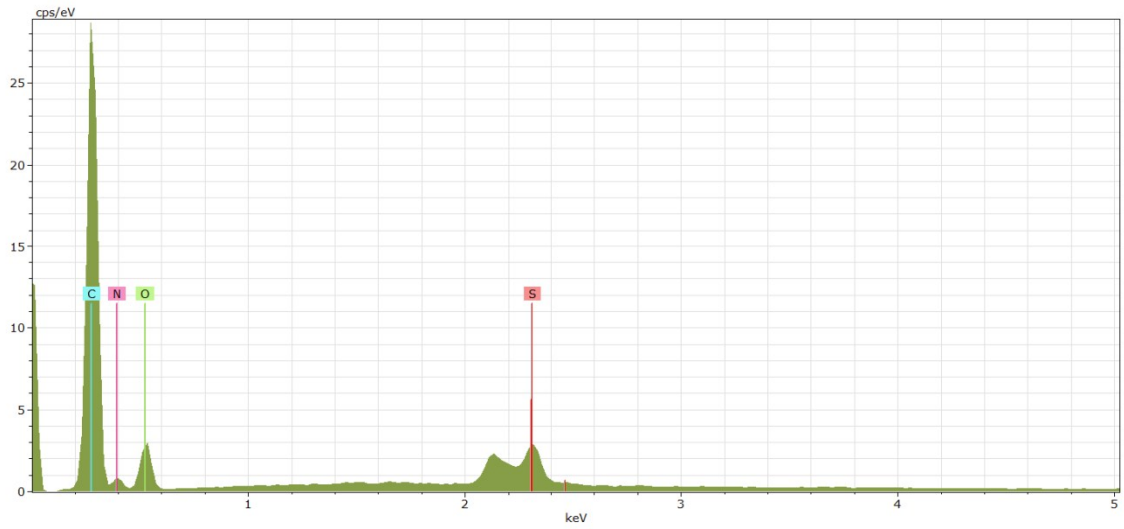

Fig. S6 Energy dispersive X-ray (EDX) spectrum of the activated MPU.

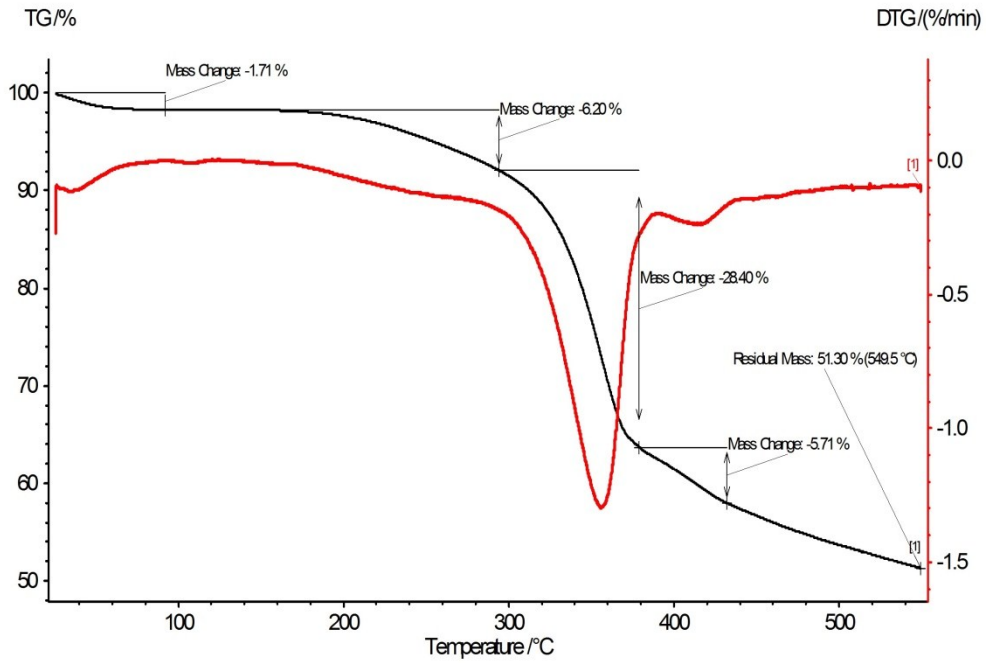

Fig. S7 Thermogravimetric (TG) curve of the activated MPU.

5. Carbon dioxide (CO_2) sorption isotherms of the MPU.

The carbon dioxide (CO_2) uptake capacity of the MPU (up to 1 bar) was 7.07 $cm^3\ g^{-1}$ (0.317 mmol g^{-1}) at 273 K and 3.27 $cm^3\ g^{-1}$ (0.146 mmol g^{-1}) at 298 K. Apart from porosity, presence of functional groups such as, -COO, -C=O, $-NH_2$ and -OH, significantly influence the CO_2 adsorption in porous materials (R. Dawson, D. J. Adams and A. I. Cooper, *Chem. Sci*., 2011, 2, 1173-1177). However, the urethane groups present along the pore walls of the MPU are possibly involved in strong interactions with the included DMSO molecules *via* amide -NH···O=S hydrogen bonding and thus, fewer polar sites are available to interact with adsorbed CO_2. Similar results (low CO_2 uptake) have recently been observed in melamine based porous organic amide polymers (S. Zulfiqar, M. I. Sarwar and C. T. Yavuz, *RSC Adv*., 2014, 4, 52263-52269).

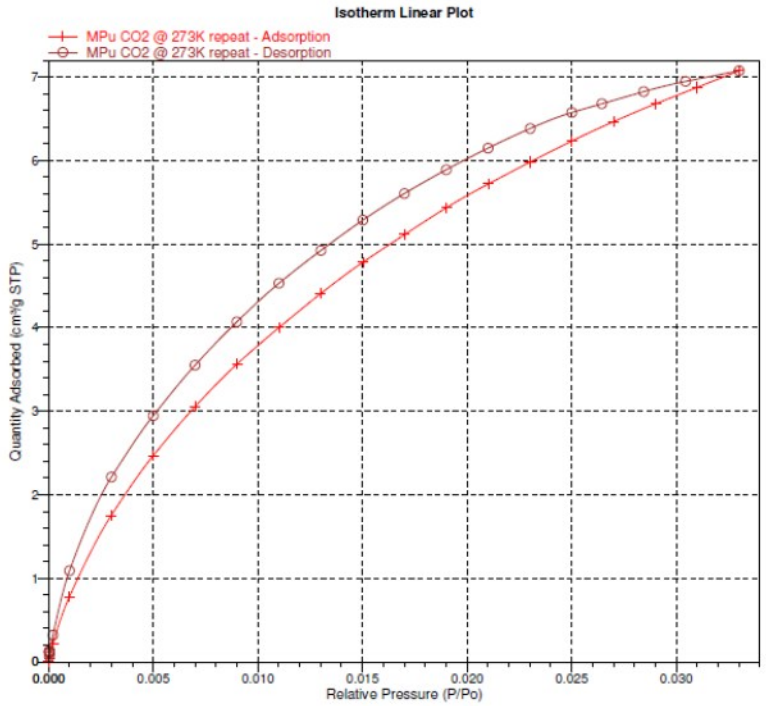

Fig. S8 CO_2 gas sorption isotherm of MPU at 273 K measured up to 1 bar pressure.

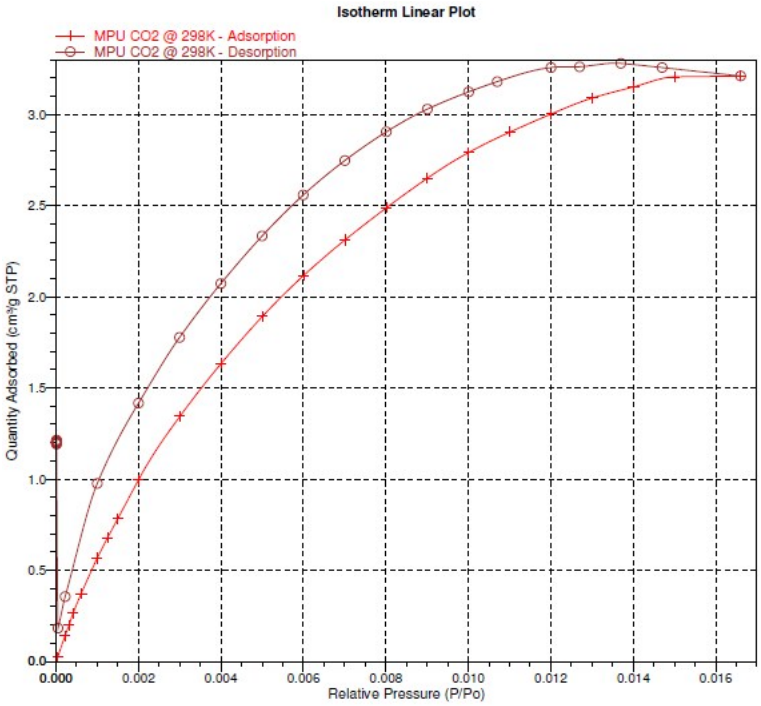

Fig. S9 CO_2 gas sorption isotherm of MPU at 298 K measured up to 1 bar pressure.

6. Potentiometric titration of MPU with 0.01 M hydrochloric acid.

To evaluate the basic property of the MPU, potentiometric titrations were carried out using 0.01 M HCl. In a typical titration procedure, 50 mg of the MPU well dispersed in 50 ml of water/ethanol was titrated against 0.01 M HCl added at a slow rate of 10 µL/min, under stirring at room temperature. However, due to the weakly basic nature of the MPU materials, no typical acid-base titration curve was obtained and thus, no clear equivalence point was detected from the curve.

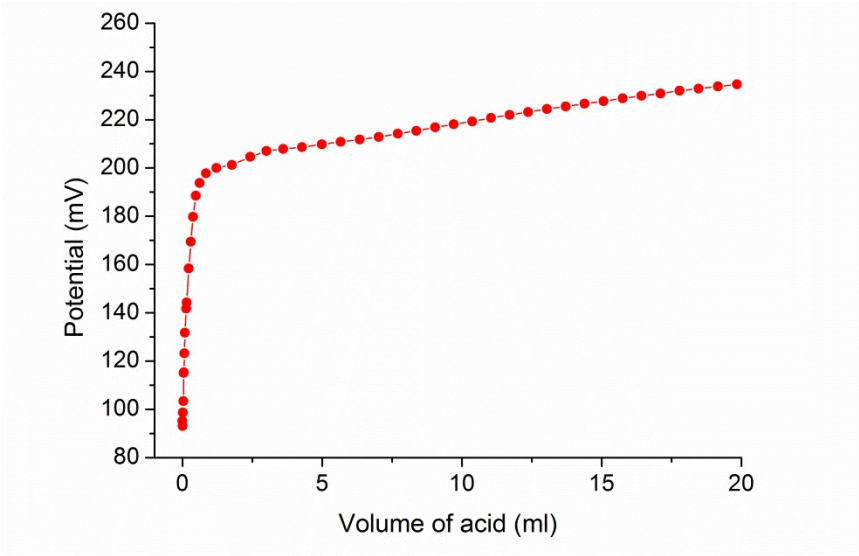

Fig. S10 Potentiometric titration curve obtained for the MPU titrating with 0.01 M HCl.

7. Characterization data of the recycled MPU.

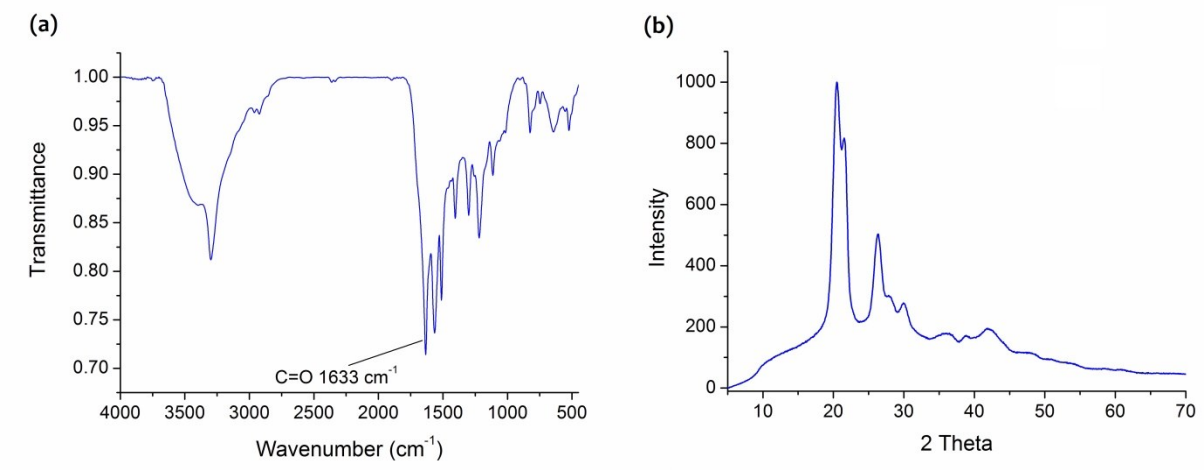

Fig. S11 (a) FT-IR spectrum and (b) PXRD pattern of the recycled MPU after first catalytic run.

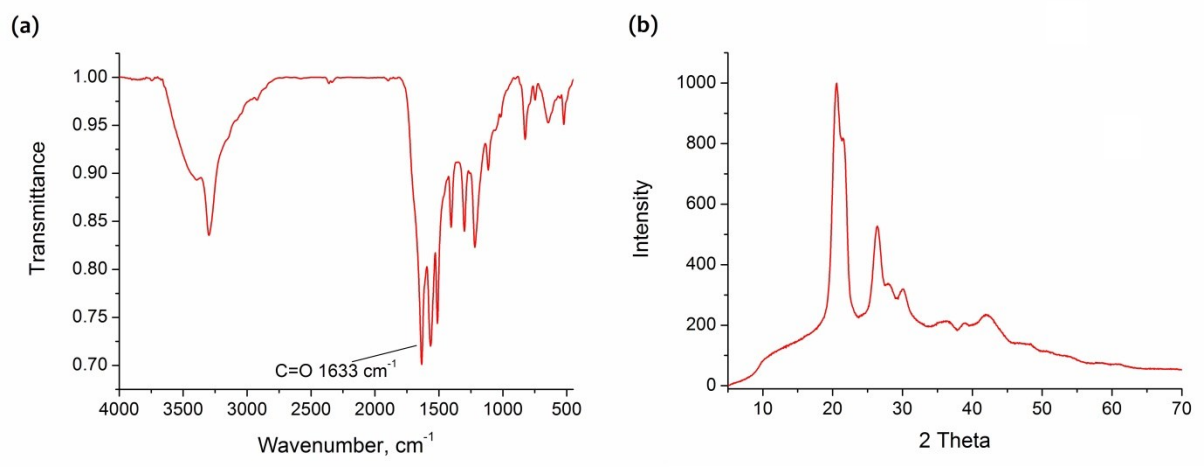

Fig. S12 (a) FT-IR spectrum and (b) PXRD pattern of the recycled MPU after second catalytic run.

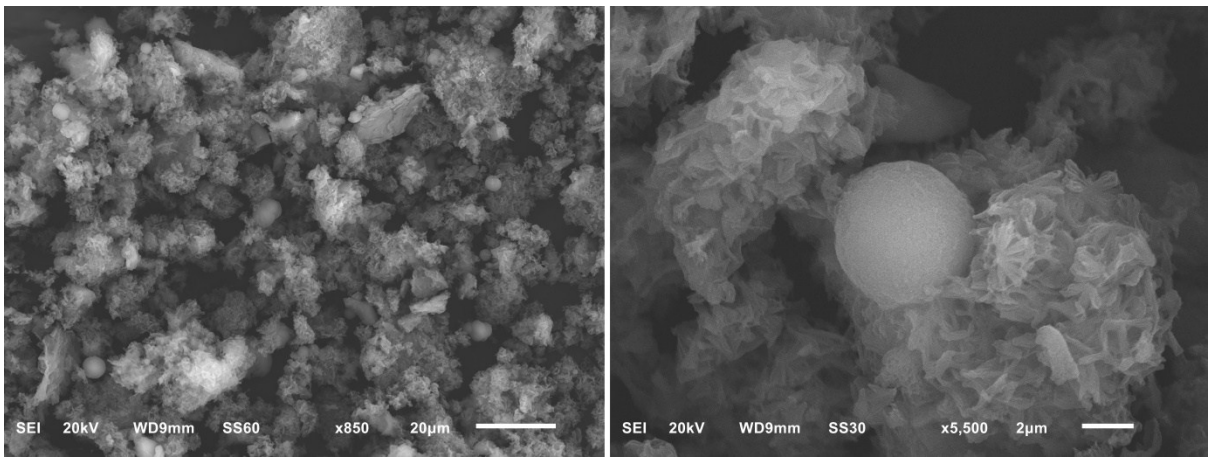

Fig. S13 Scanning electron microscope (SEM) images of the recycled MPU after catalysis.

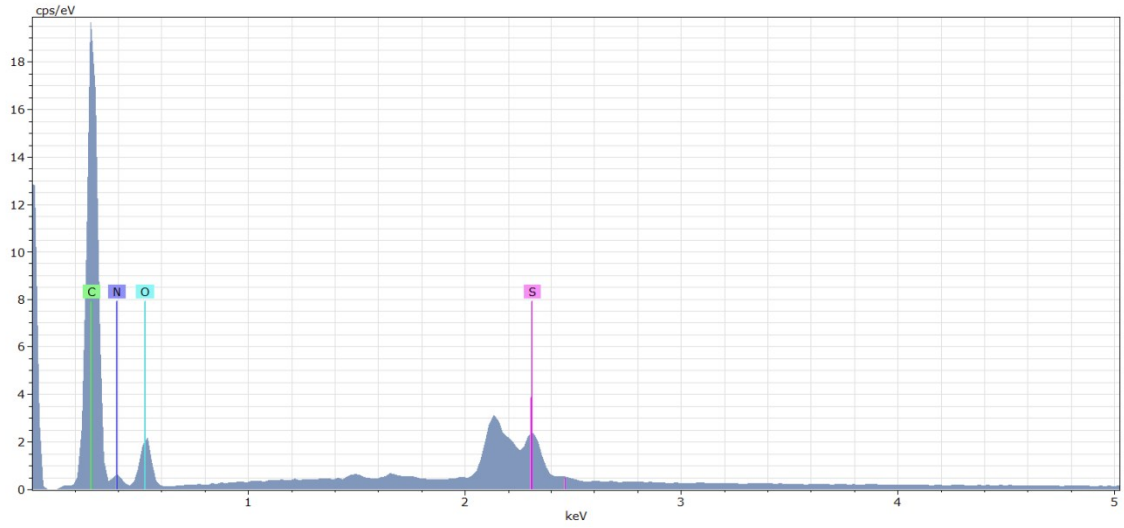

Fig. S14 Energy dispersive X-ray (EDX) spectrum of the recycled MPU after catalysis.

8. Conversion (%) Vs Time (h) plot of the MPU catalysed Knoevenagel reaction.

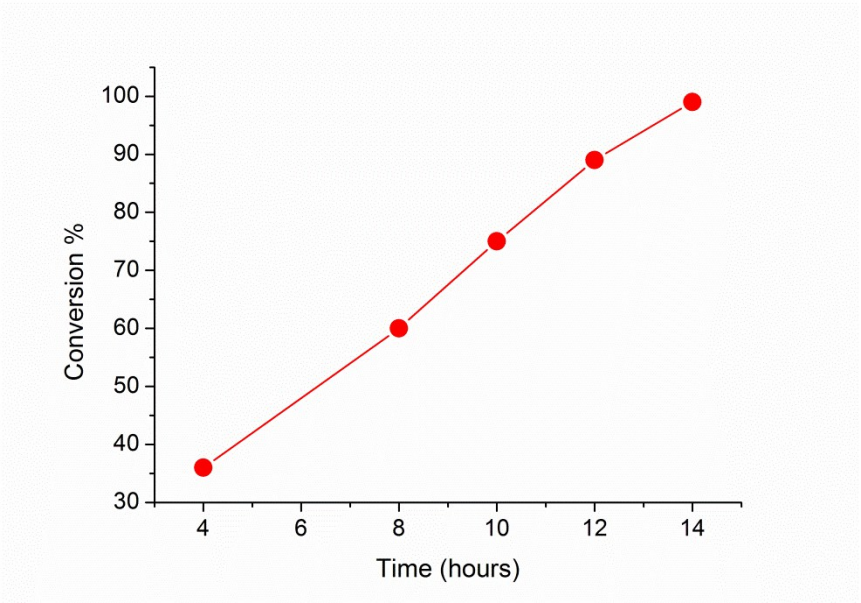

Fig. S15 Conversion vs Time plot for the Knoevenagel reaction between benzaldehyde (1.0 mmol) and malononitrile (1.1 mmol) in the presence of 5 mol% (18 mg) of MPU at 50 °C in THF.

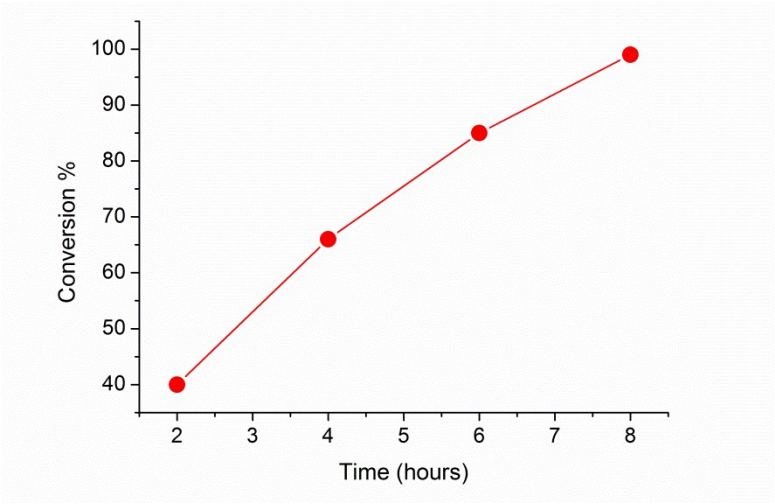

Fig. S16 Conversion vs Time plot for the Knoevenagel reaction between benzaldehyde (1.0 mmol) and malononitrile (2.0 mmol) in the presence of 5 mol% (18 mg) of MPU at 50 °C in THF.

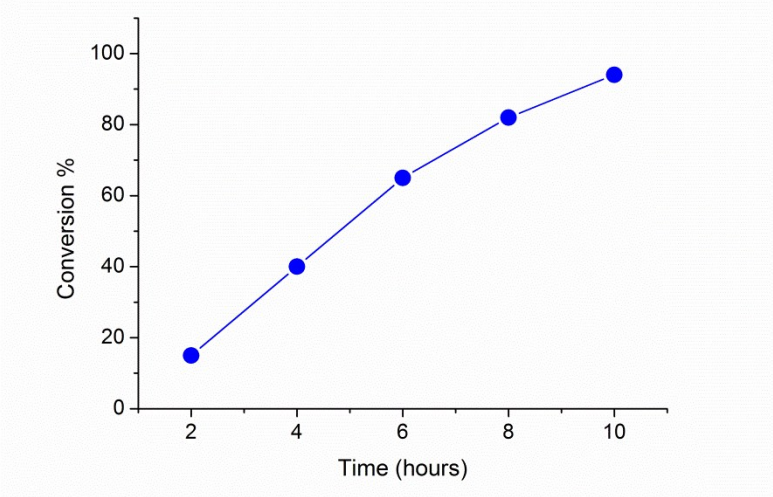

Fig. S17 Conversion vs Time plot for the Henry reaction between benzaldehyde (1.0 mmol) and nitromethane (10 mmol) in the presence of 5 mol% (18 mg) of MPU at 50 °C in methanol.

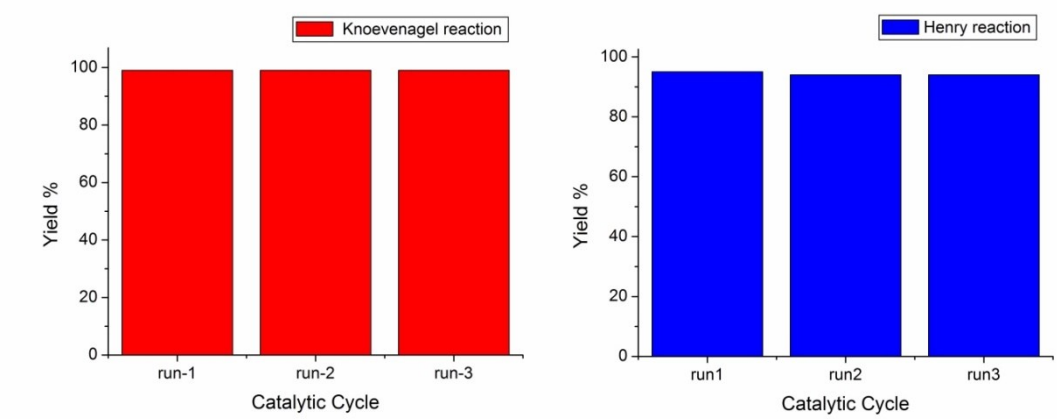

Fig. S18 Catalyst recycling studies for the Knoevenagel reaction between 4-nitrobenzaldehyde and malononitrile, and for the Henry reaction between 4-nitrobenzaldehyde and nitromethane.

9. Hot filtration tests (Leaching tests) for Knoevenagel and Henry reactions

Hot filtration tests in the Knoevenagel and Henry reactions have been performed for the model reactions between benzaldehyde and malononitrile/nitromethane. The detailed kinetic study of the Knoevenagel reaction between benzaldehyde and malononitrile showed that the MPU catalysed reaction is completed within 14 h at 50 °C in THF, monitored by ^{1}H NMR spectroscopy at regular intervals of time (4 h, 8 h, 10 h, 12 h, and 14 h) (Fig. S15). In the hot filtration test, the organic phase was separated from the solid catalyst after 4 h reaction time by simple filtration, having used 5 mol % of the MPU catalyst. A portion of the filtrate was pipetted out, dried under reduced pressure and analysed by ^{1}H NMR spectroscopy, which showed 38% product formation to benzylidenemalononitrile (Fig. S19). In the meantime, the bulk catalyst free solution was transferred to a new reactor vessel, and heated at 50 °C for an additional 10 h. The reaction solution was then evaporated under reduced pressure, dried and analysed by ^{1}H NMR spectroscopy. Within experimental error, about 40% yield was obtained after 14 h, proving that there was no contribution from leached active species and that conversion was only possible in the presence of the solid MPU catalyst.

The detailed kinetic study of the Henry reaction between 4-nitrobenzaldehyde and nitromethane showed that the MPU catalysed reaction is completed within 10 h at 50 °C in methanol, to give 94% yield. Unlike the Knoevenagel reaction, the nitroaldol reaction between 4-nitrobenzaldehyde and nitromethane did not proceed in THF signifying the importance of protic solvent in the MPU catalysed Henry reaction. Similar to the Knoevenagel reaction, the reaction mixture was separated from the solid catalyst after 4 h reaction time by simple filtration, having used 5 mol % of the MPU catalyst. A portion of the filtrate was pipetted out, dried under reduced pressure and analysed by ^{1}H NMR spectroscopy, which showed 40% product formation (Fig. S20). In the meantime, the bulk catalyst free solution was transferred to a new reactor vessel, and heated at 50 °C for an additional 6 h. The reaction solution was then evaporated under reduced pressure, dried and analysed by ^{1}H NMR spectroscopy, which showed an increase of about 5-10% yield possibly due to the protic nature of the reaction medium or some nanoparticular catalyst material. Still, after a further reaction time of 6 h the yield increased only to 45-50% (up from 40% after 4 h) which is well below 94% in the presence of solid MPU catalyst.

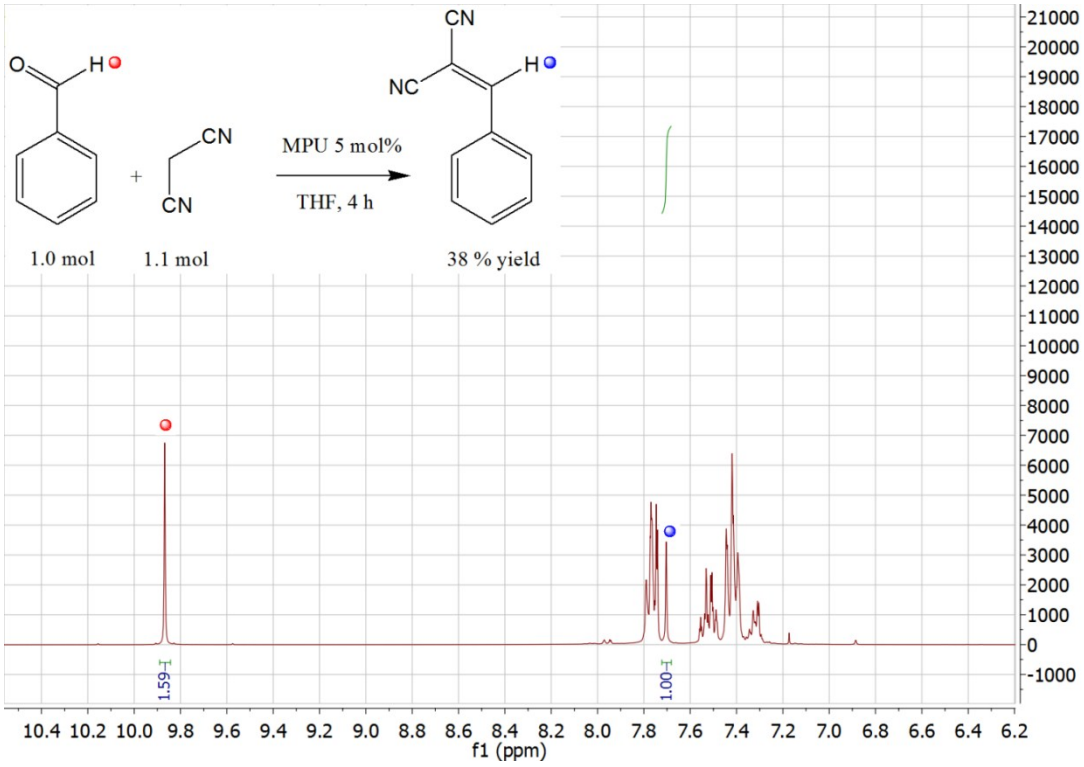

Fig. S19 ^{1}H NMR spectrum ($CDCl_3$, aromatic region) of the model reaction between benzaldehyde and malononitrile in THF at 50 °C for 4 h, showing 38% conversion to benzylidenemalononitrile.

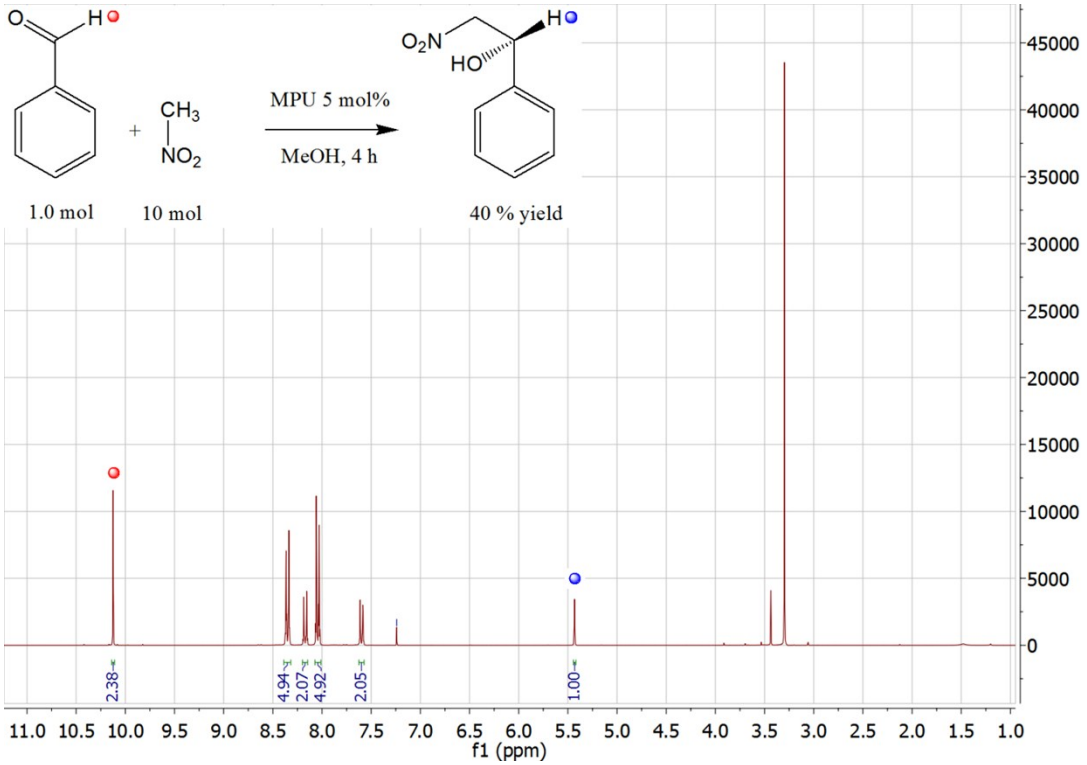

Fig. S20 ^{1}H NMR spectrum ($CDCl_3$) of the model reaction between benzaldehyde and nitromethane in methanol at 50 °C for 4 h, showing 40% conversion to β-nitroalkanol.

10. Characterization of the Knoevenagel reaction products by NMR.

Activated MPU catalysed Knoevenagel reaction of malononitrile with various aromatic aldehydes.

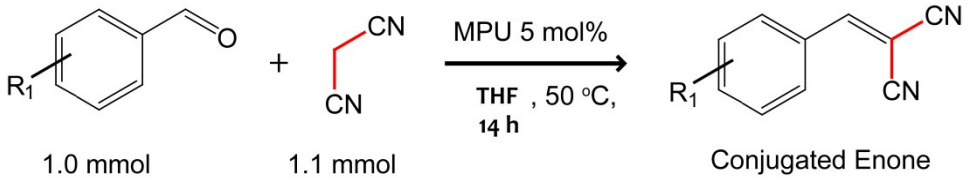

Yields are calculated with respect to the unreacted aldehydes present in the reaction mixture (see the ^{1}H NMR spectral analysis, Fig S42-S49)

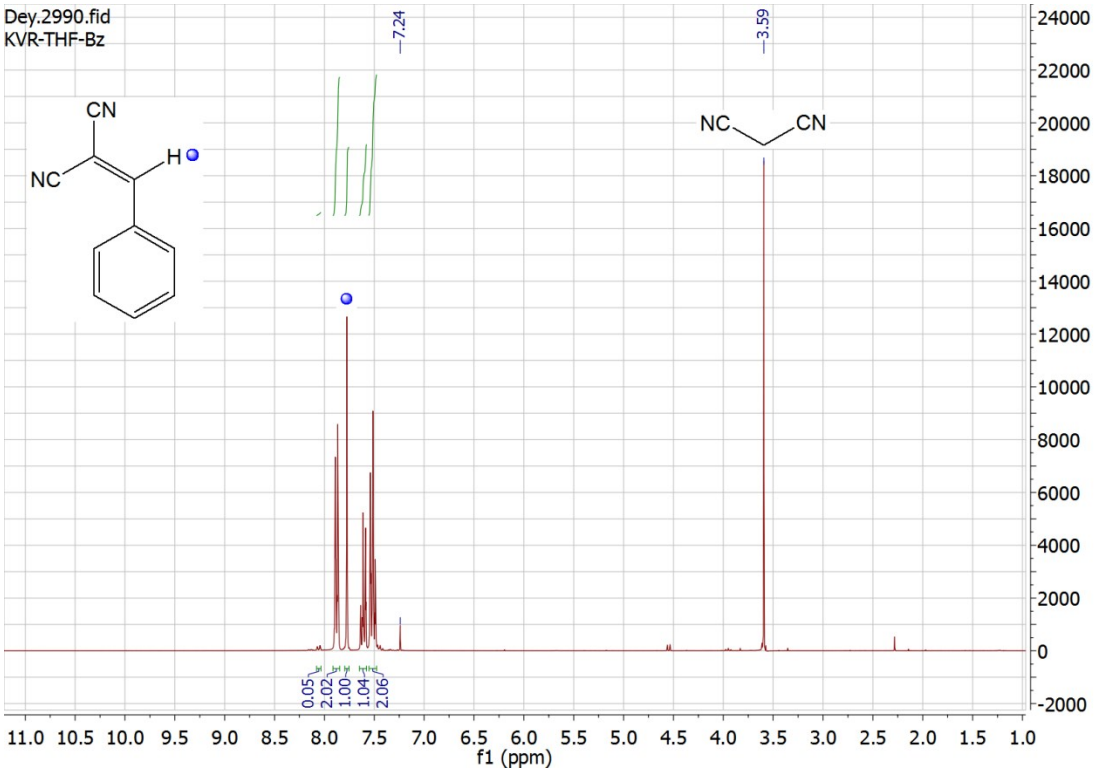

Fig. S21 ^{1}H NMR spectrum of as synthesized benzylidenemalononitrile in $CDCl_3$. The peak at 3.59 corresponds to excess malononitrile.

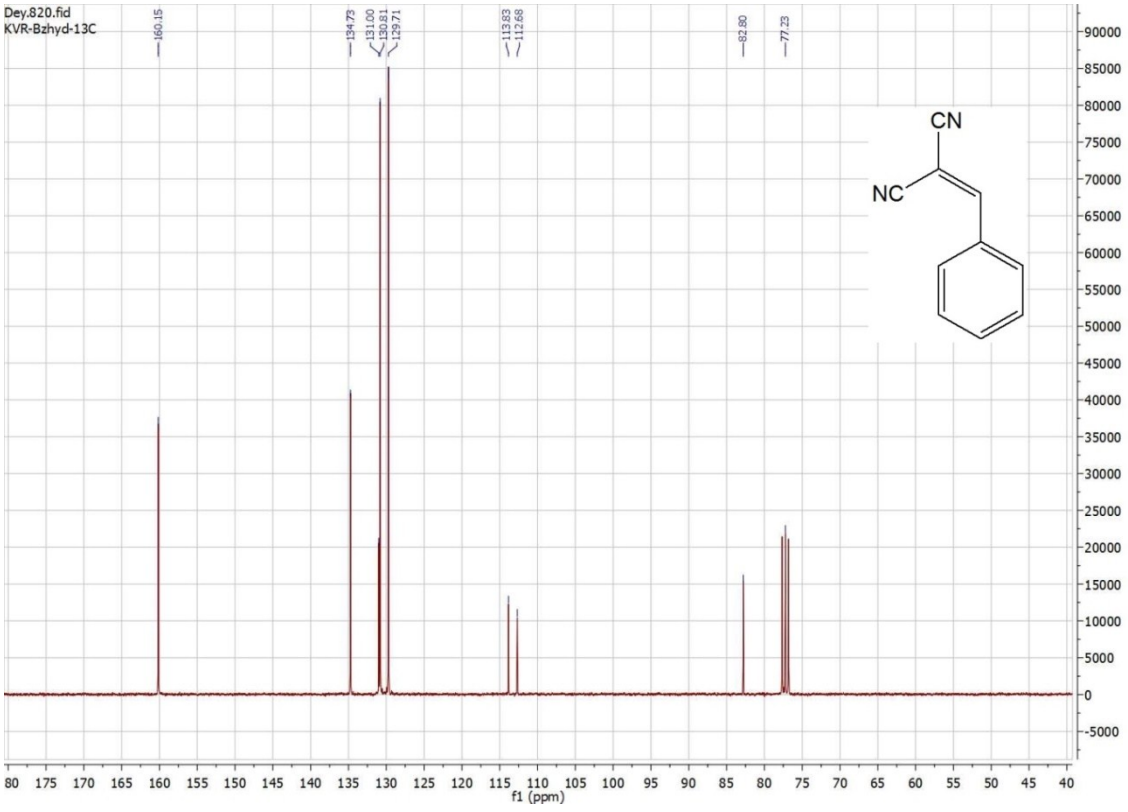

Fig. S22 ^{13}C NMR spectrum of pure benzylidenemalononitrile (recrystallized from MeOH) in $CDCl_3$.

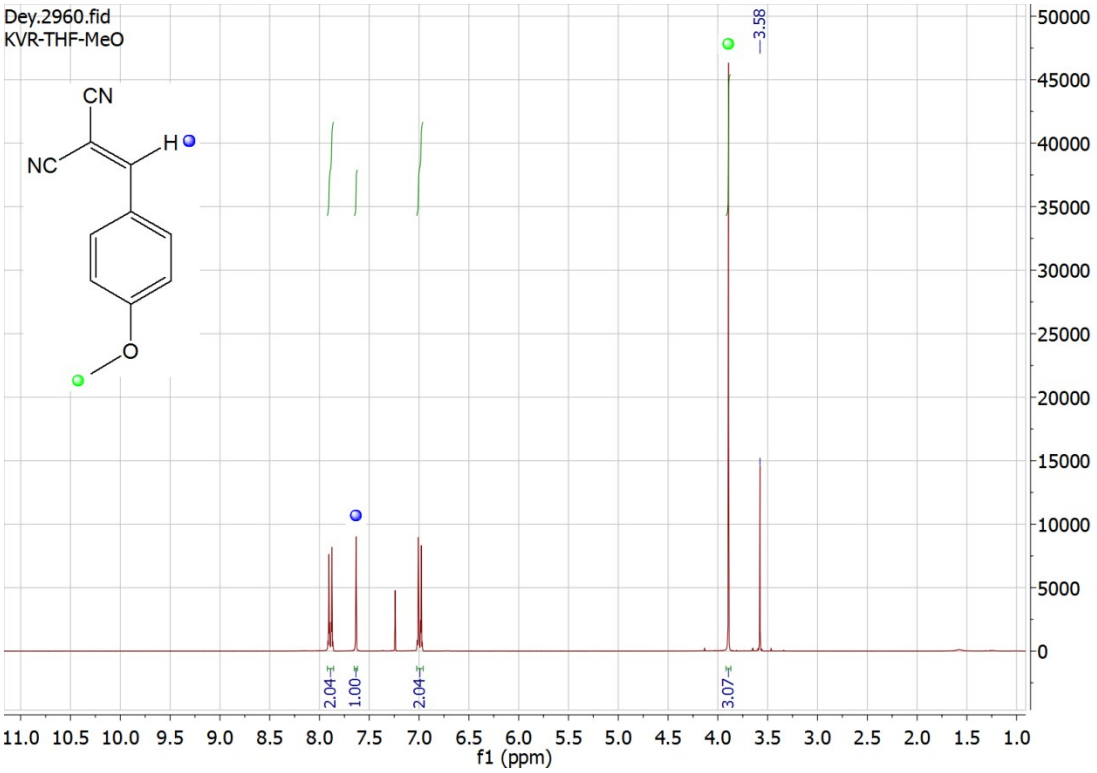

Fig. S23 ^{1}H NMR spectrum of as synthesized (4-methoxybenzylidene)malononitrile in $CDCl_3$. The peak at 3.58 corresponds to excess malononitrile.

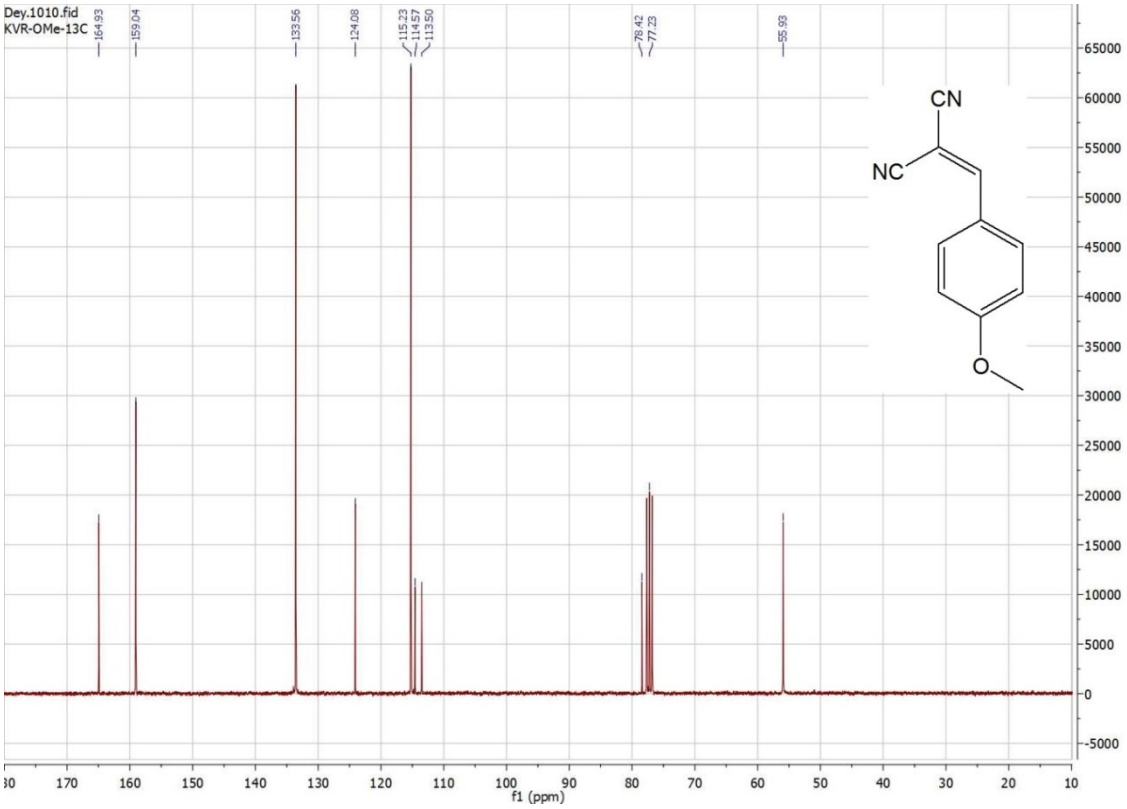

Fig. S24 ^{13}C NMR spectrum of pure (4-methoxybenzylidene)malononitrile (recrystallized from MeOH) in $CDCl_3$.

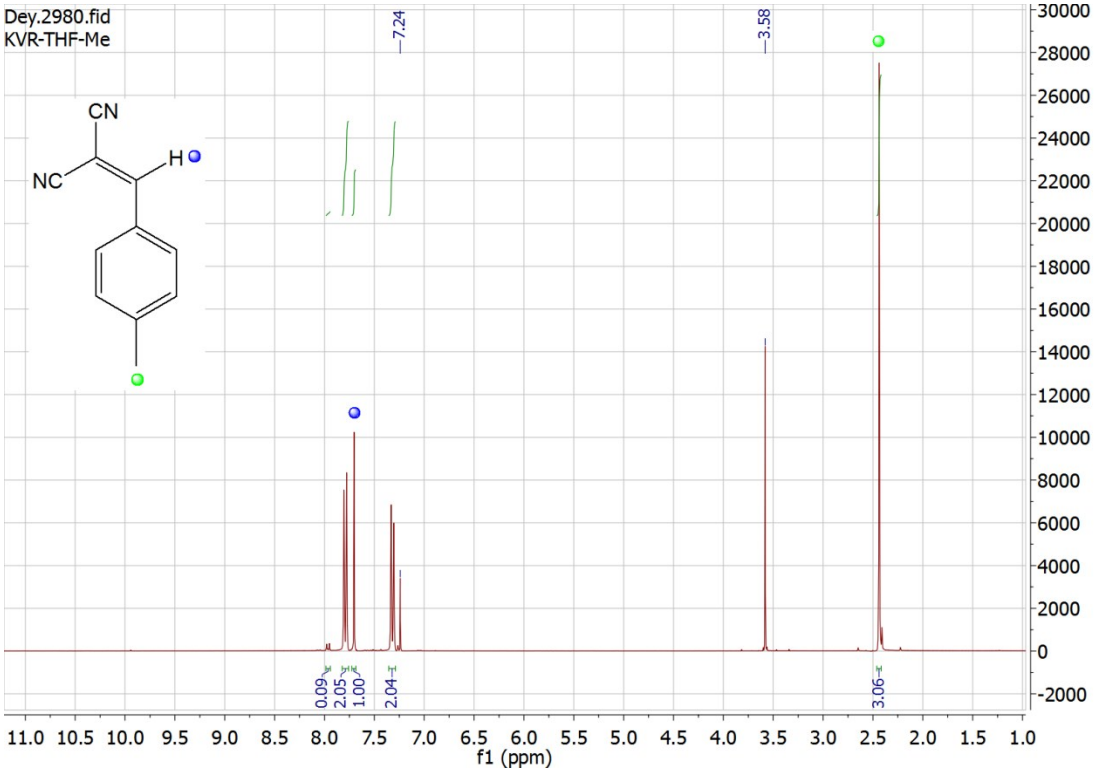

Fig. S25 ^{1}H NMR spectrum of as synthesized (4-methylbenzylidene)malononitrile in $CDCl_3$. The peak at 3.58 corresponds to excess malononitrile.

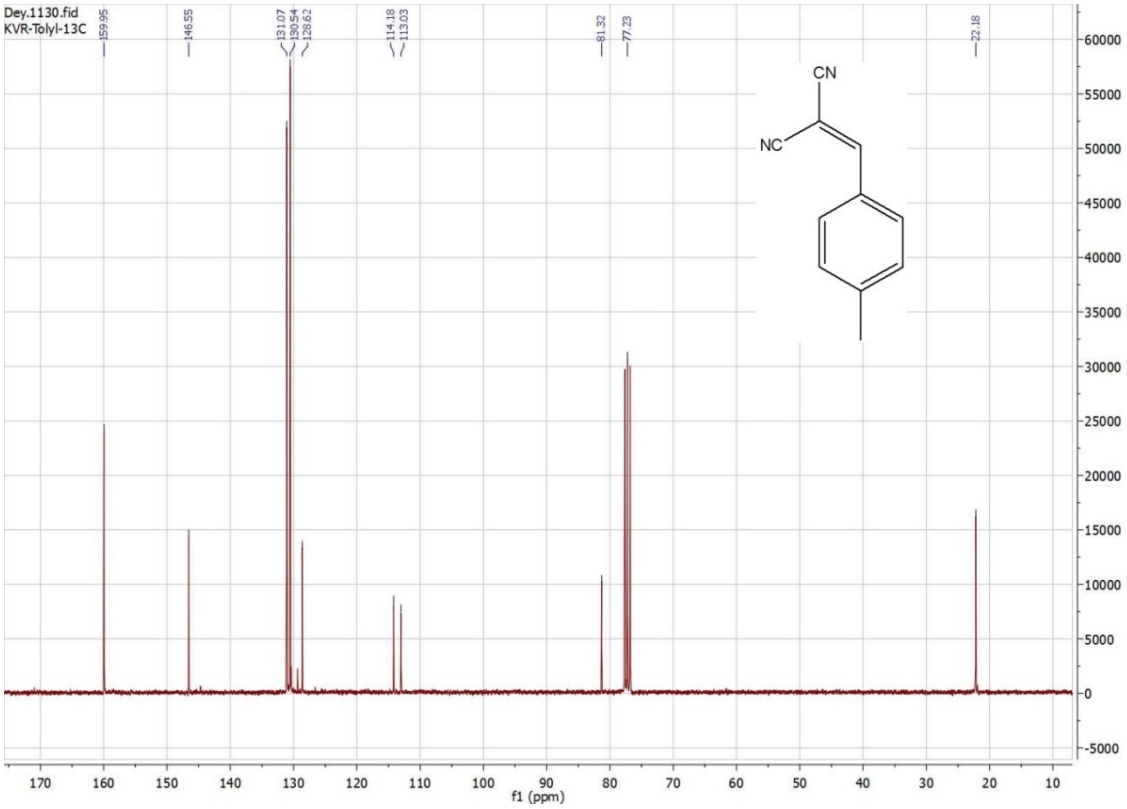

Fig. S26 ^{13}C NMR spectrum of pure (4-methylbenzylidene)malononitrile (recrystallized from MeOH) in $CDCl_3$.

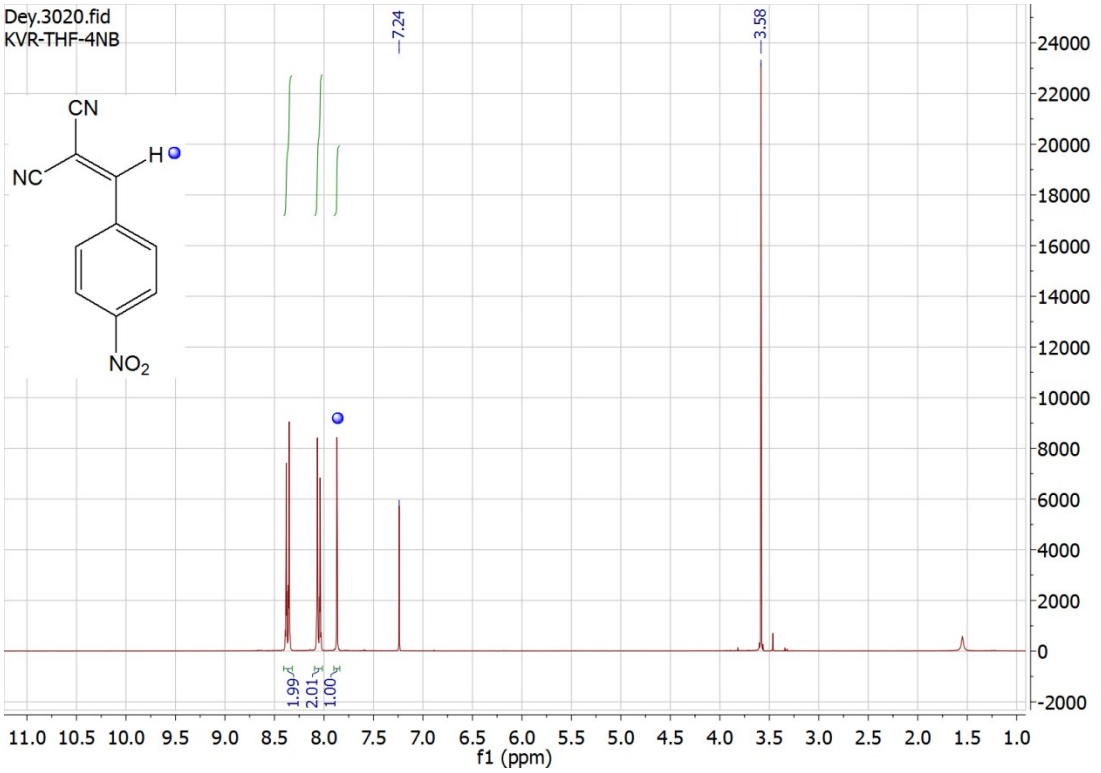

Fig. S27 ^{1}H NMR spectrum of as synthesized (4-nitrobenzylidene)malononitrile in $CDCl_3$. The peak at 3.58 corresponds to excess malononitrile.

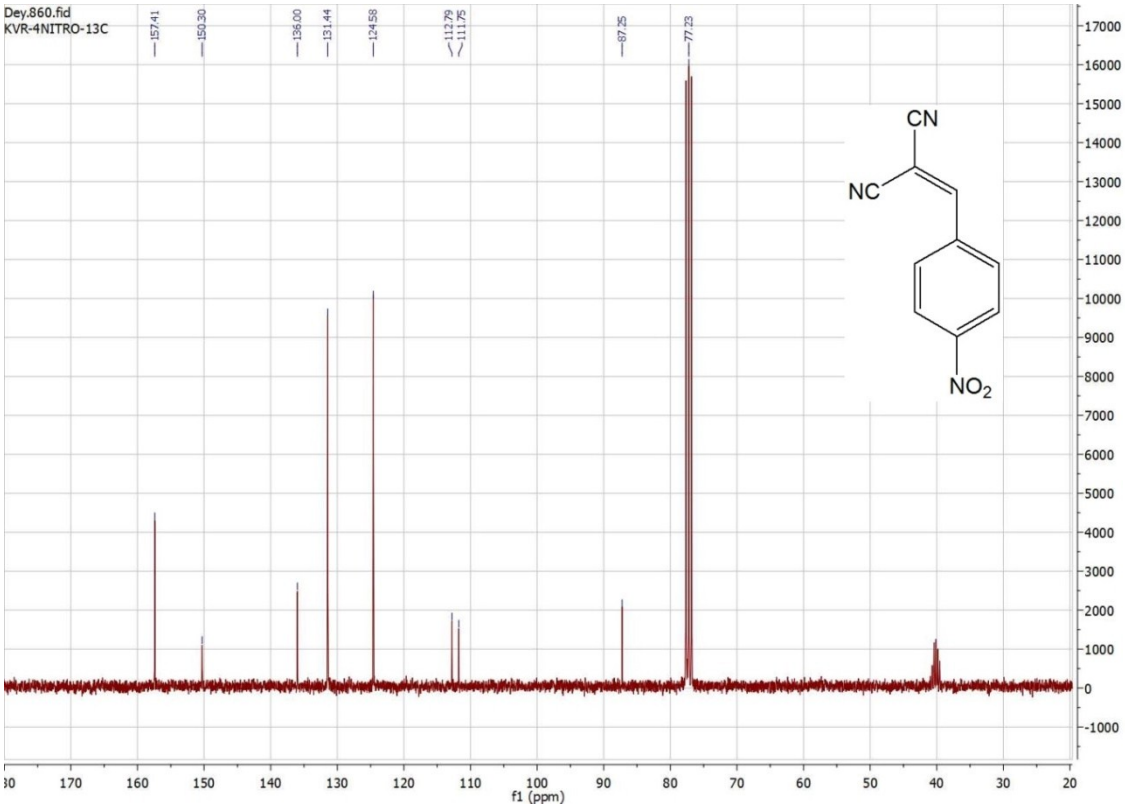

Fig. S28 ^{13}C NMR spectrum of pure (4-nitrobenzylidene)malononitrile (recrystallized from MeOH) in $CDCl_3$.

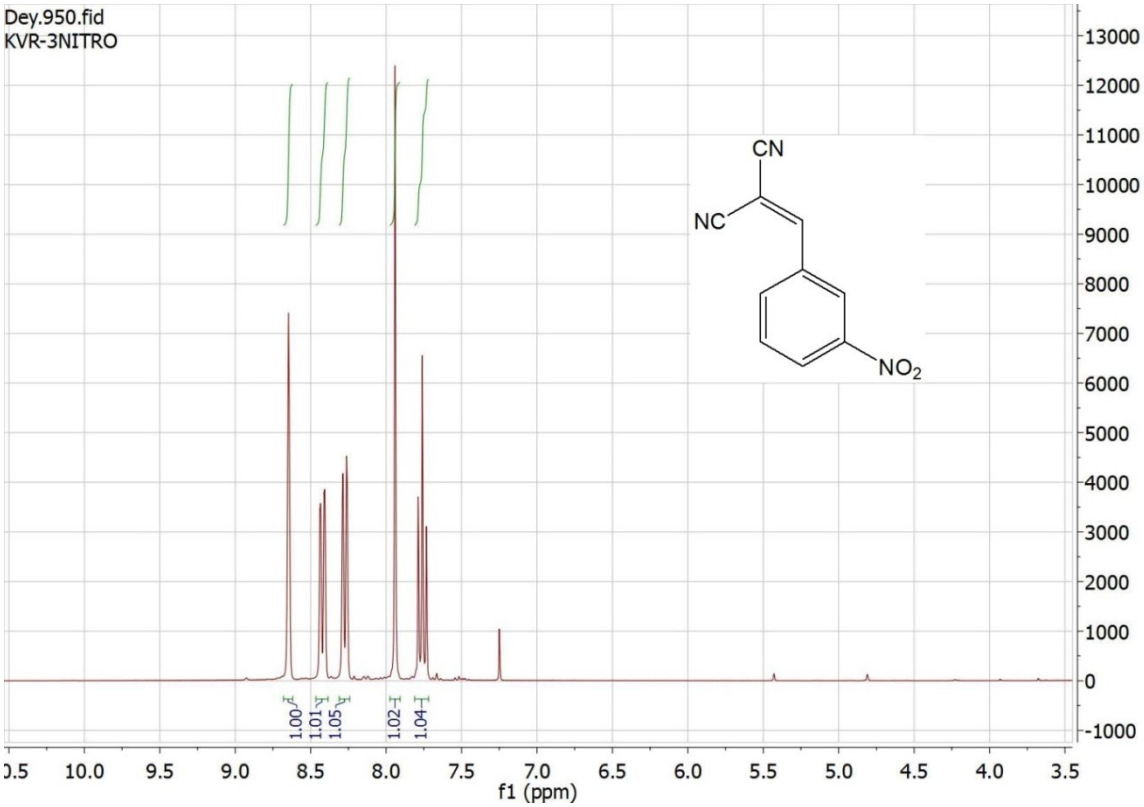

Fig. S29 ^{1}H NMR spectrum of as synthesized (3-nitrobenzylidene)malononitrile in $CDCl_3$.

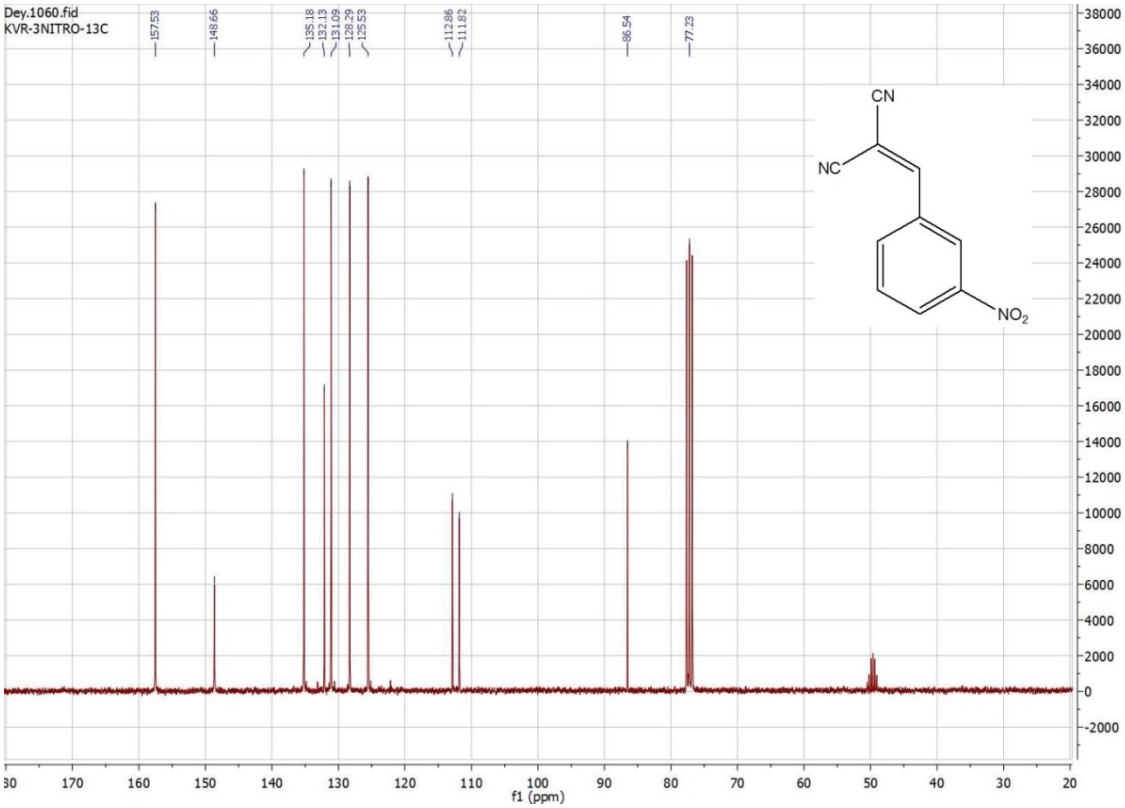

Fig. S30 ^{13}C NMR spectrum of pure (3-nitrobenzylidene)malononitrile (recrystallized from MeOH) in $CDCl_3$.

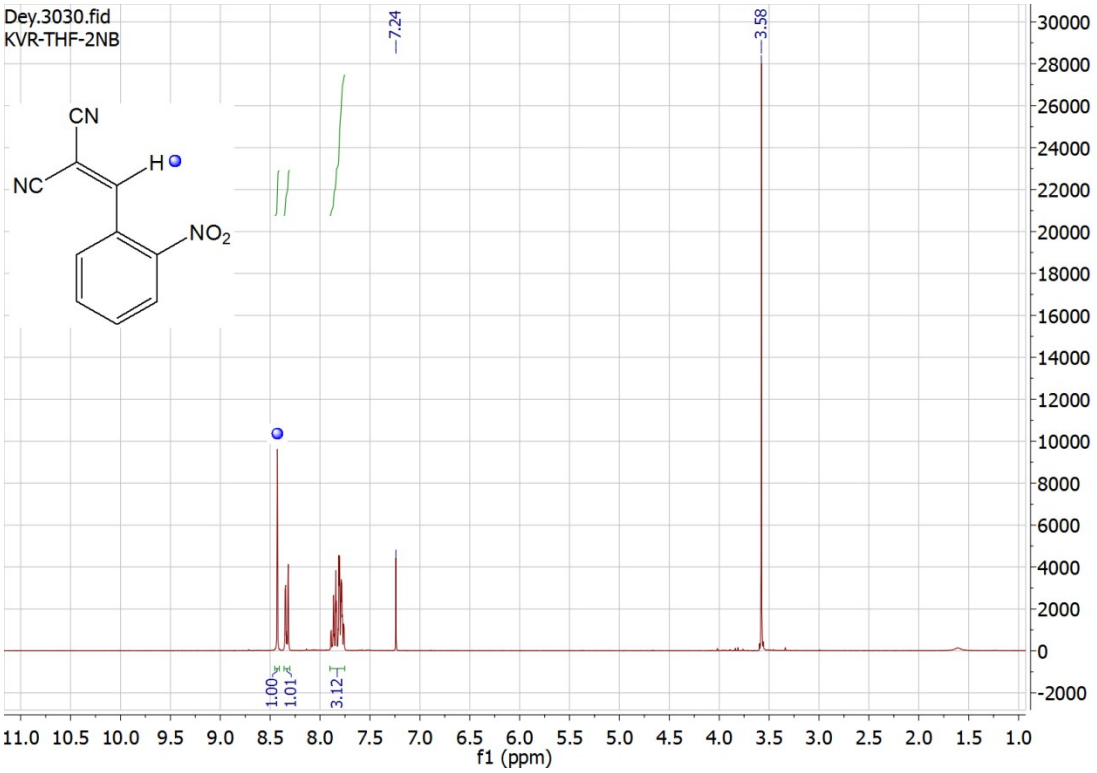

Fig. S31 ^{1}H NMR spectrum of as synthesized (2-nitrobenzylidene)malononitrile in $CDCl_3$. The peak at 3.58 corresponds to excess malononitrile.

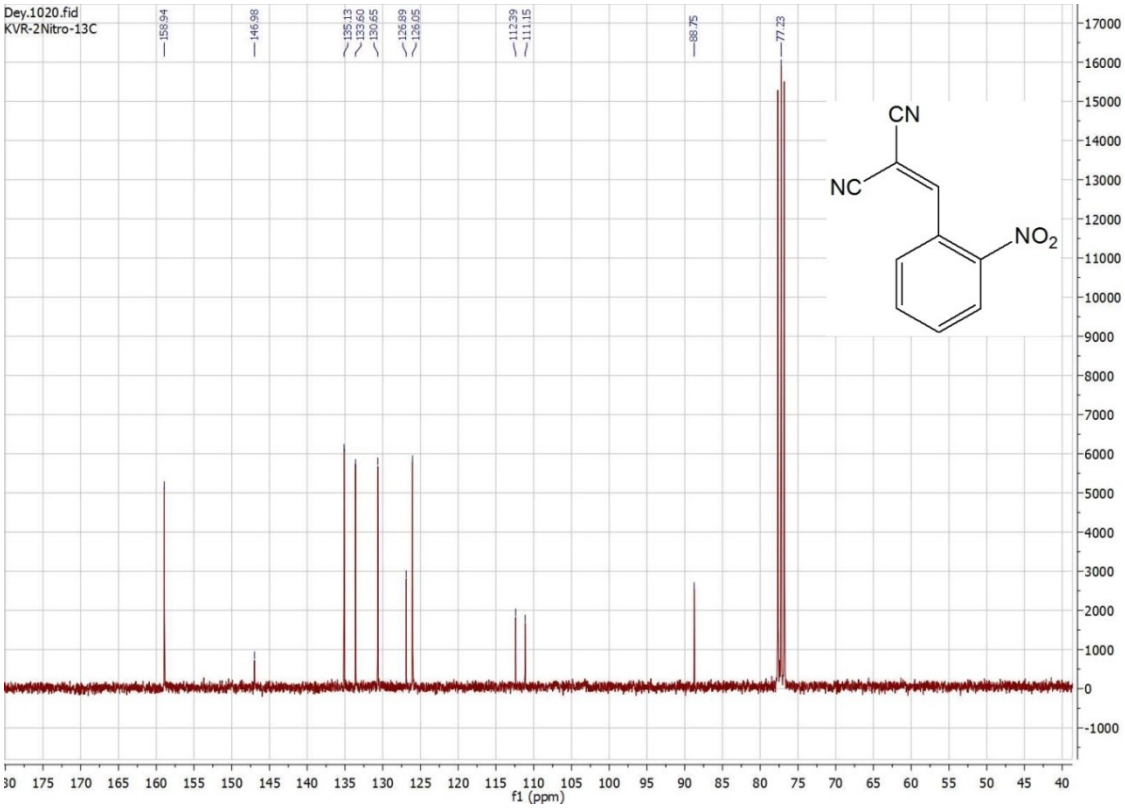

Fig. S32 ^{13}C NMR spectrum of pure (2-nitrobenzylidene)malononitrile (recrystallized from MeOH) in $CDCl_3$.

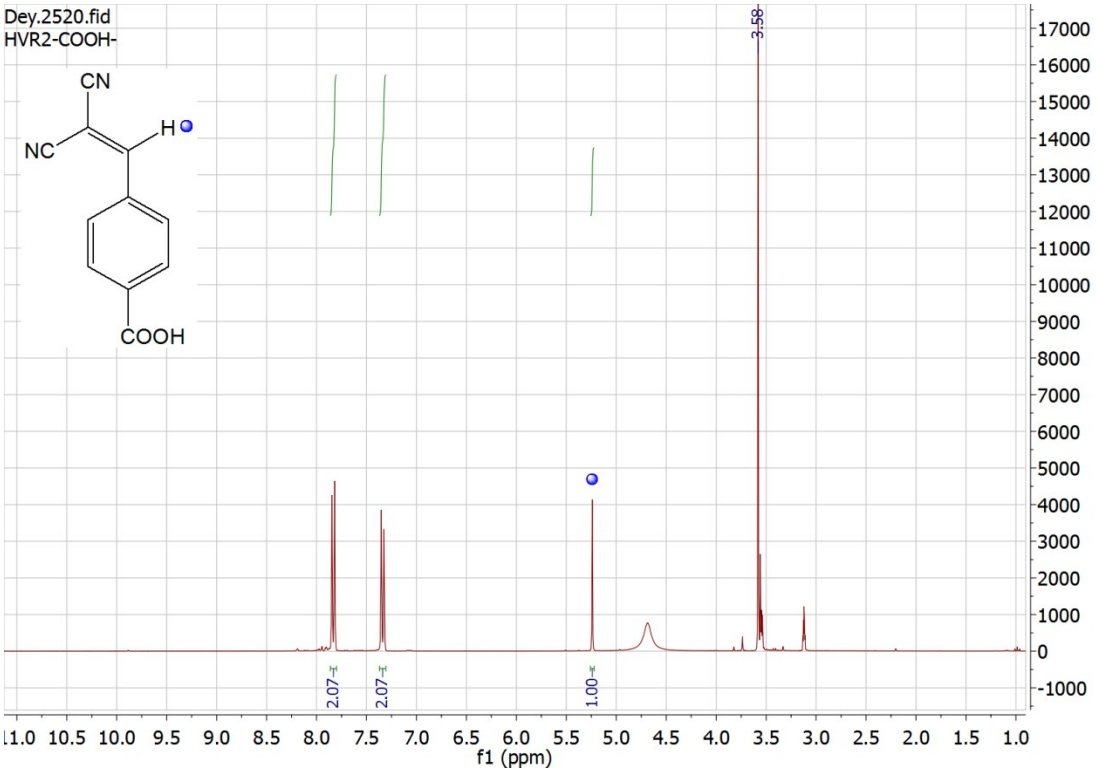

Fig. S33 ^{1}H NMR spectrum of as synthesized (4-carboxybenzylidene)malononitrile in $CDCl_3$. The peak at 3.58 corresponds to excess malononitrile.

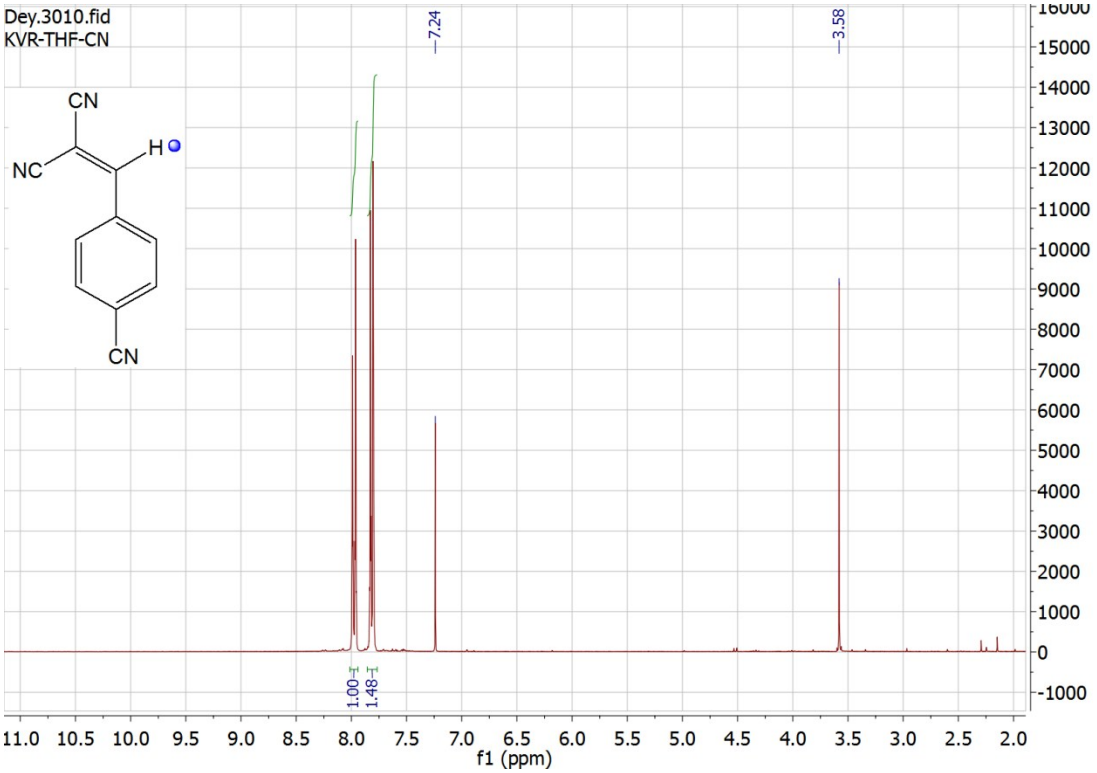

Fig. S34 ^{1}H NMR spectrum of as synthesized (4-cyanobenzylidene)malononitrile in $CDCl_3$. The peak at 3.58 corresponds to excess malononitrile.

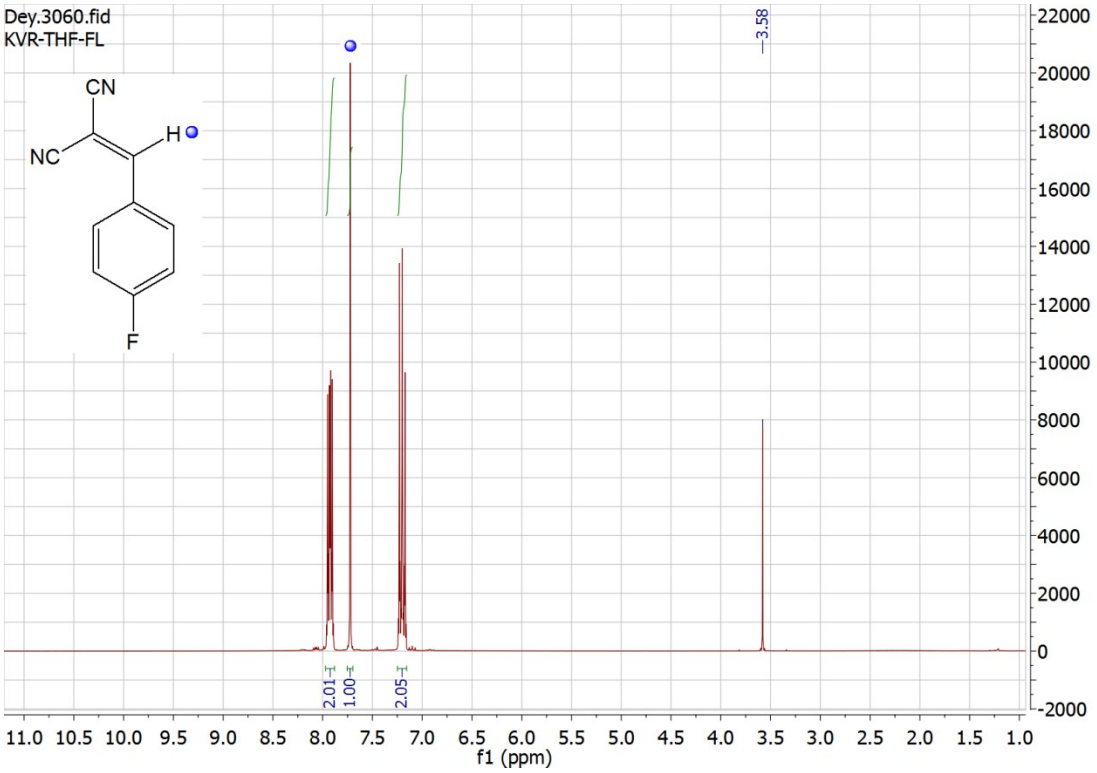

Fig. S35 ^{1}H NMR spectrum of as synthesized (4-fluorobenzylidene)malononitrile in $CDCl_3$. The peak at 3.58 corresponds to excess malononitrile.

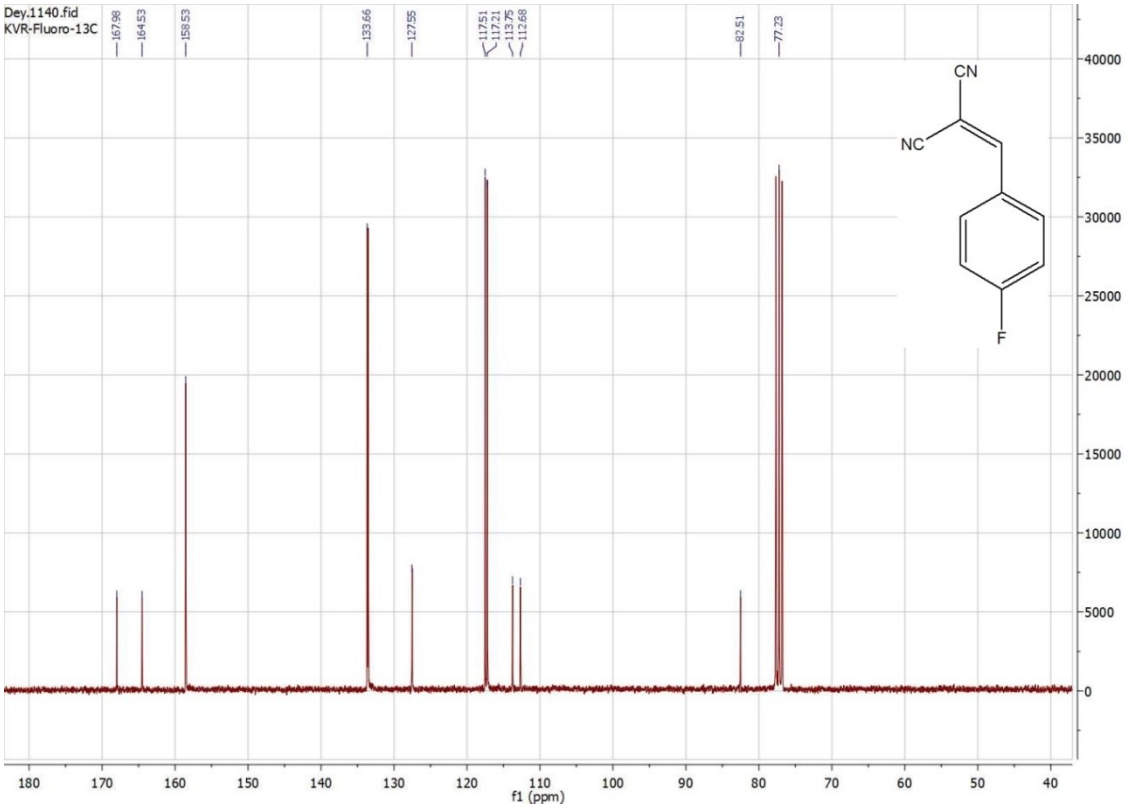

Fig. S36 ^{13}C NMR spectrum of pure (4-fluorobenzylidene)malononitrile (recrystallized from MeOH) in $CDCl_3$.

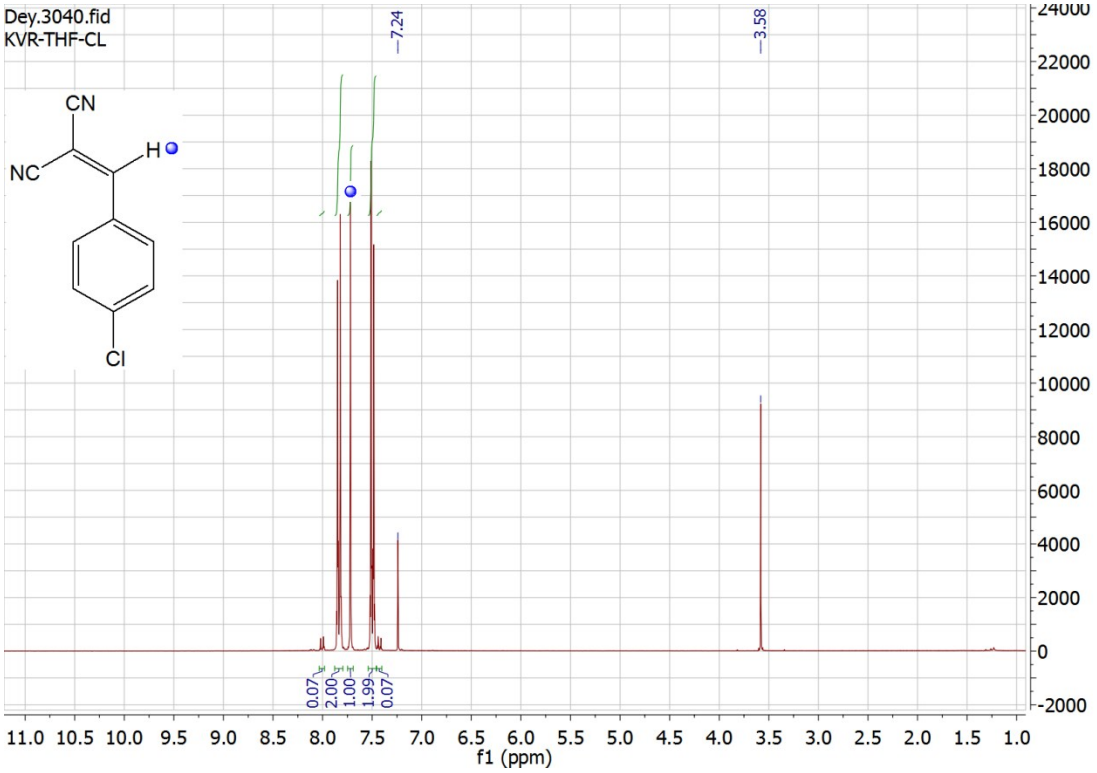

Fig. S37 ^{1}H NMR spectrum of as synthesized (4-chlorobenzylidene)malononitrile in $CDCl_3$. The peak at 3.58 corresponds to excess malononitrile.

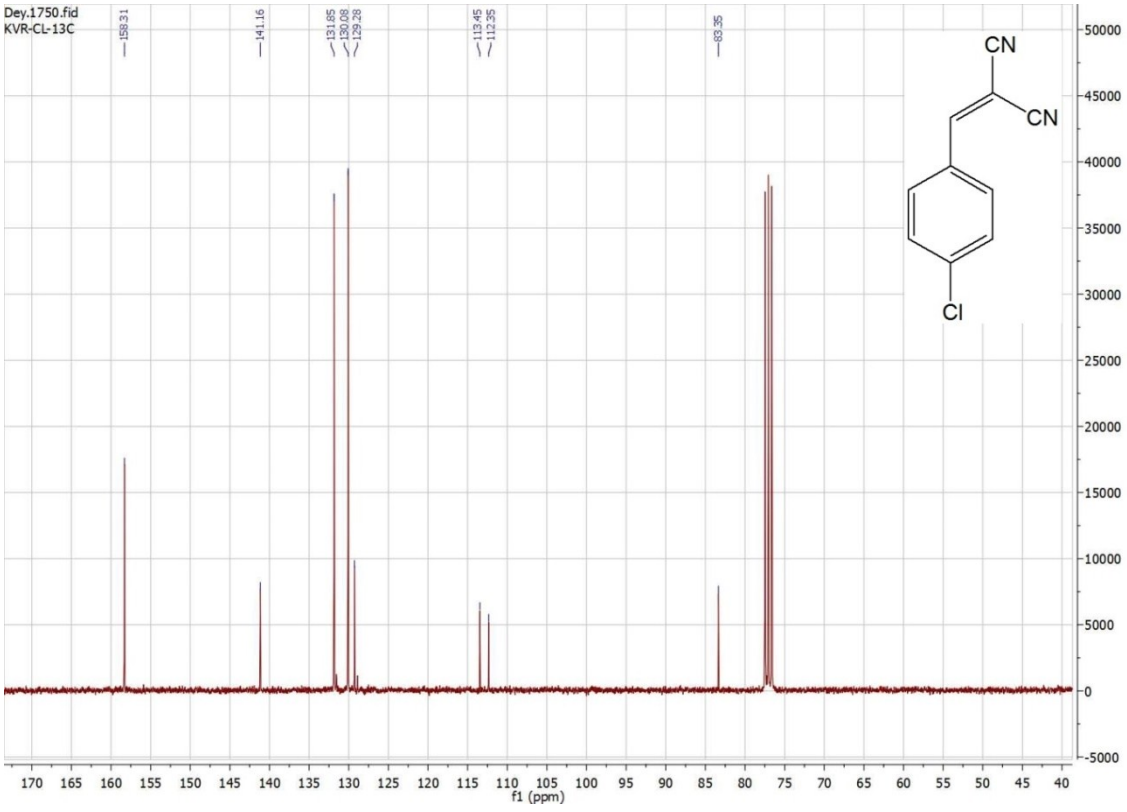

Fig. S38 ^{13}C NMR spectrum of pure (4-chlorobenzylidene)malononitrile (recrystallized from MeOH) in $CDCl_3$.

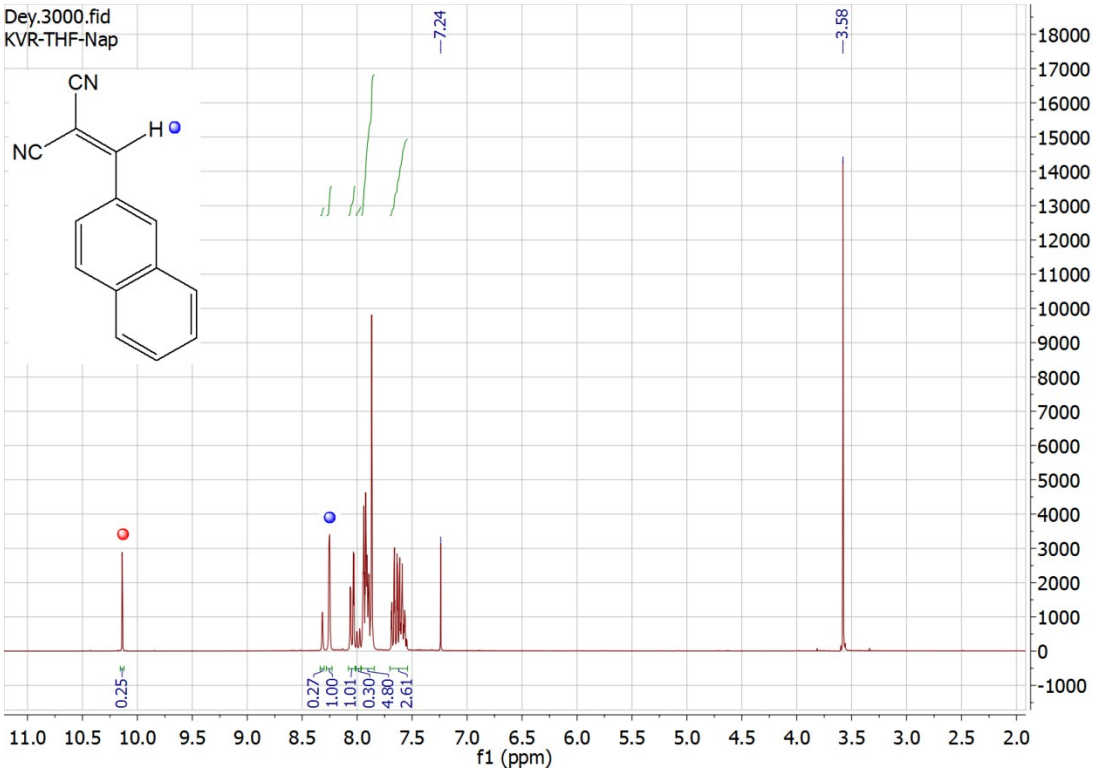

Fig. S39 ^{1}H NMR spectrum of crude 2-(naphthalen-2-ylmethylene)malononitrile in $CDCl_3$. The peak at 3.58 corresponds to excess malononitrile and the peak marked with red circle represents unreacted naphthaldehyde –CHO proton.

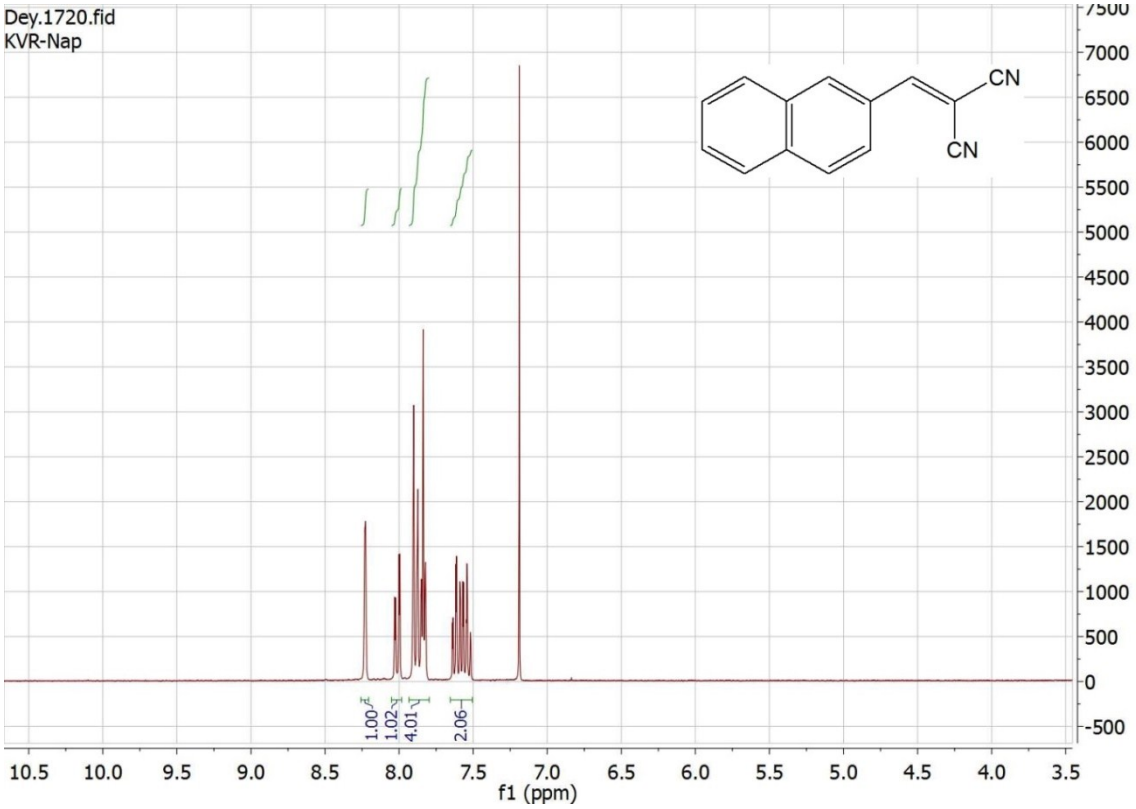

Fig. S40 ^{1}H NMR spectrum of pure 2-(naphthalen-2-ylmethylene)malononitrile (recrystallized from MeOH) in $CDCl_3$.

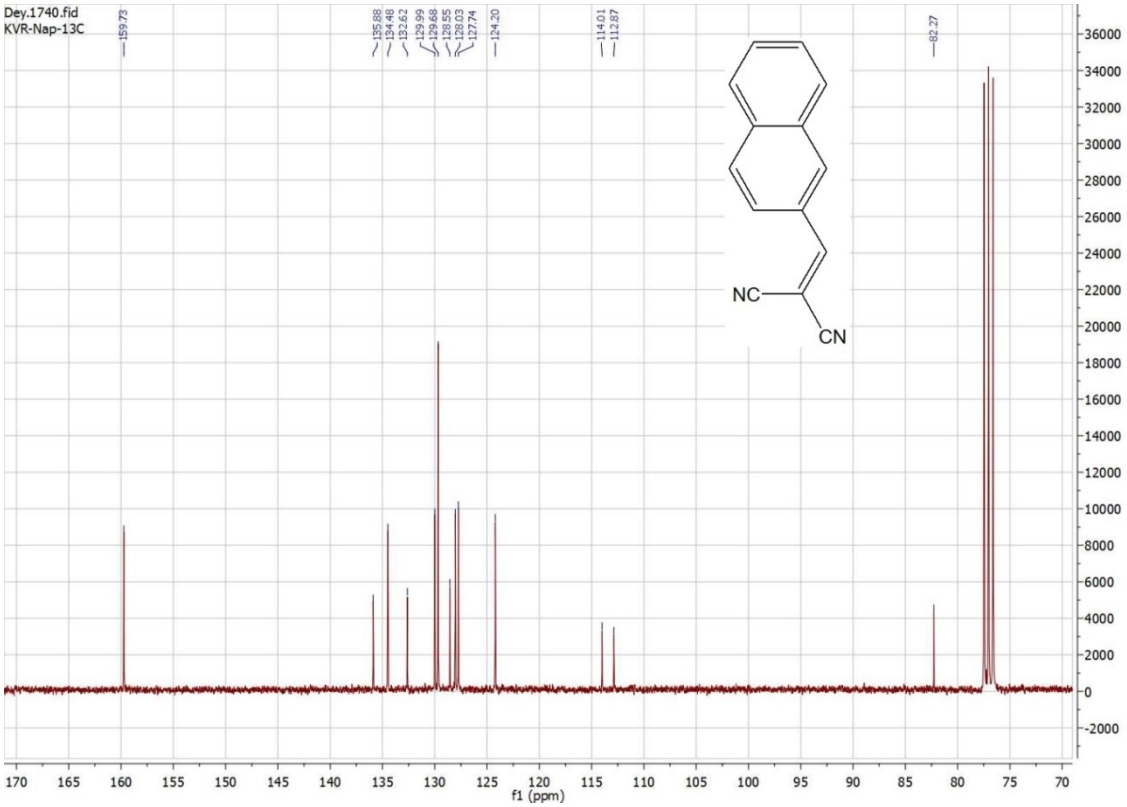

Fig. S41 ^{13}C NMR spectrum of pure 2-(naphthalen-2-ylmethylene)malononitrile in $CDCl_3$.

Activated MPU catalysed Knoevenagel reaction of methylcyanoacetate with various aromatic aldehydes in THF.

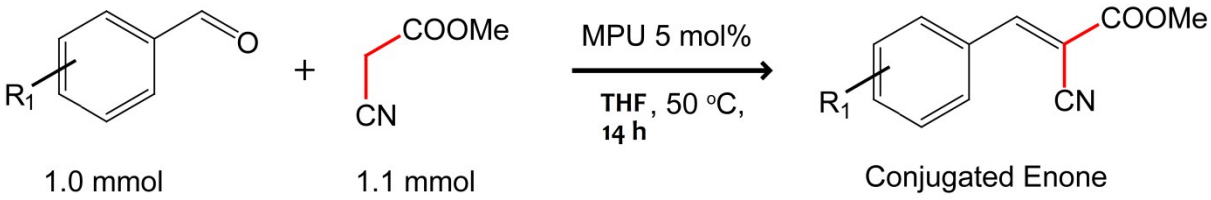

Yields are calculated with respect to the unreacted aldehydes present in the reaction mixture (see the ^{1}H NMR spectral analysis, Fig S42-S49)

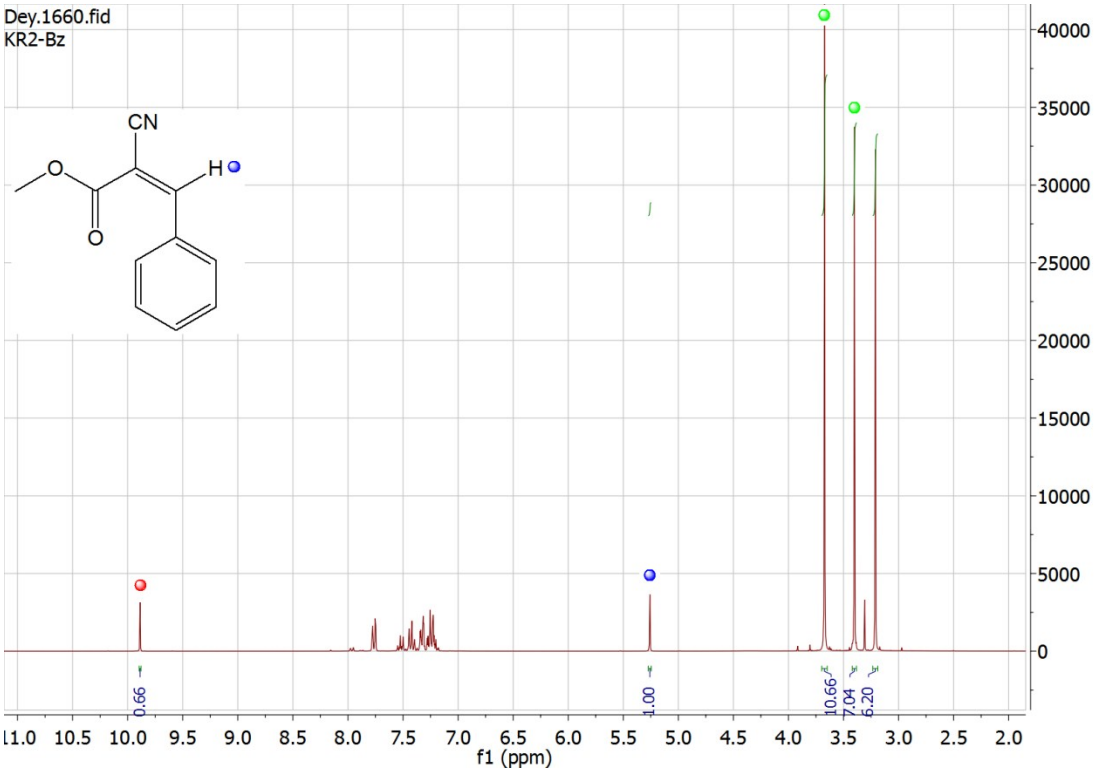

Fig. S42 1H NMR spectrum of as synthesized 2-cyano-3-(phenyl)methylacrylate in CDCl3. Signals for unreacted aldehyde and methylcyanoacetate are represented with red and green circles, respectively.

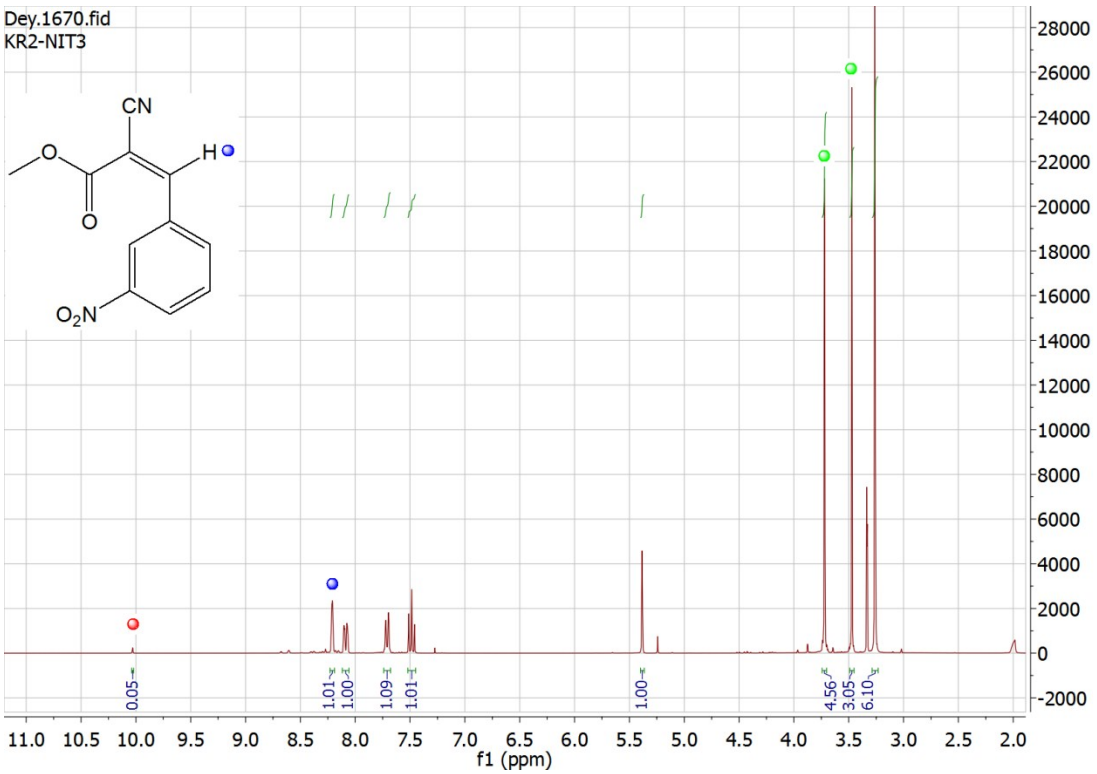

Fig. S42 ^{1}H NMR spectrum of as synthesized 2-cyano-3-(3-nitrophenyl)methylacrylate in $CDCl_3$. Signals for unreacted aldehyde and methylcyanoacetate are represented with red and green circles, respectively.

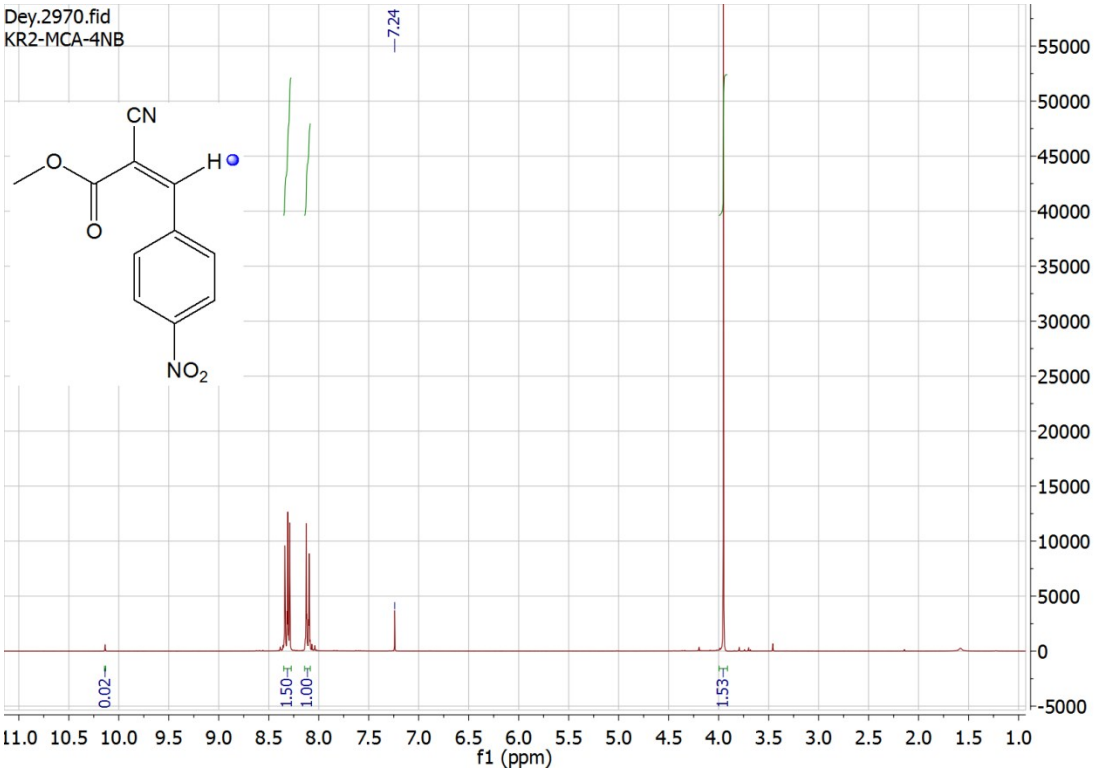

Fig. S43 ^{1}H NMR spectrum of as synthesized 2-cyano-3-(4-nitrophenyl)methylacrylate in $CDCl_3$.

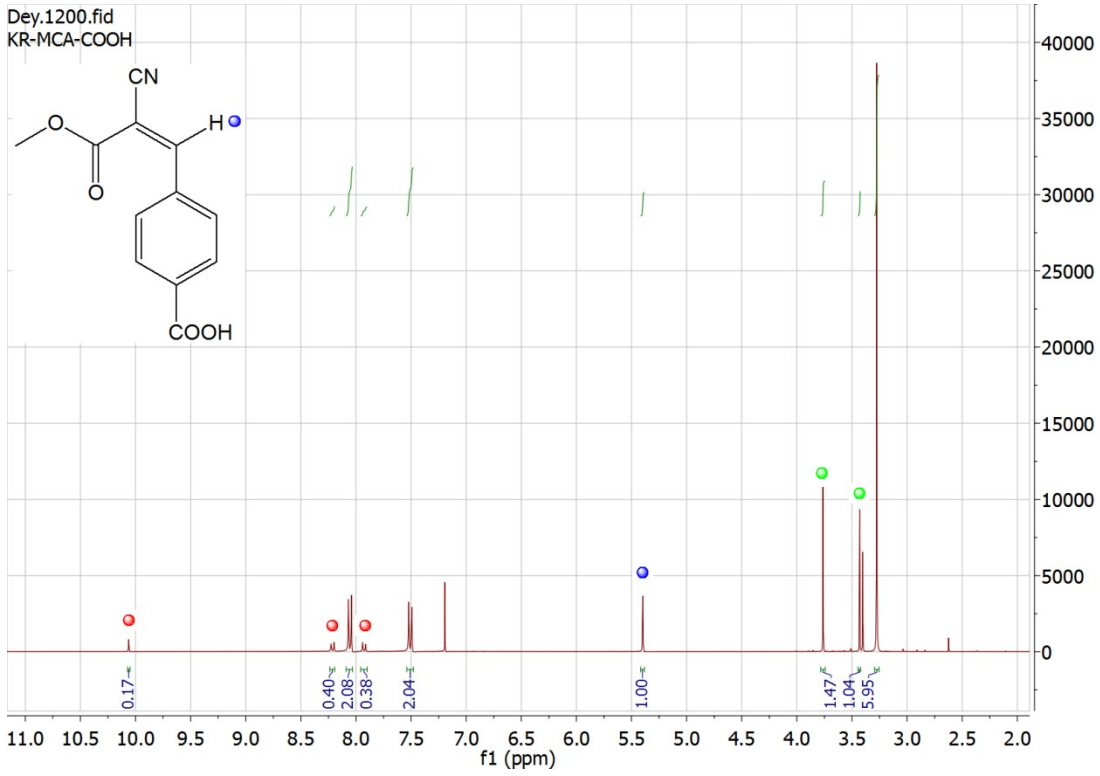

Fig. S44 ^{1}H NMR spectrum of as synthesized 2-cyano-3-(4-carboxyphenyl)methylacrylate in $CDCl_3$. Signals for unreacted aldehyde and methylcyanoacetate are represented with red and green circles, respectively.

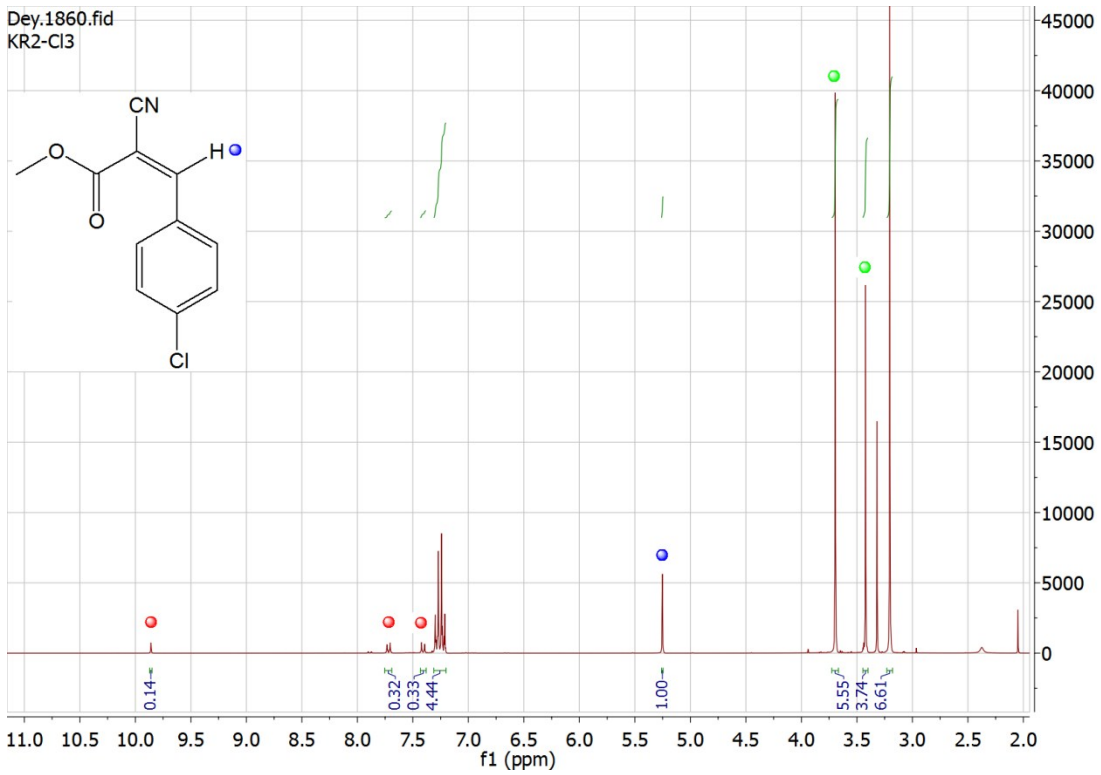

Fig. S45 ^{1}H NMR spectrum of as synthesized 2-cyano-3-(4-chlorophenyl)methylacrylate in $CDCl_3$. Signals for unreacted aldehyde and methylcyanoacetate are represented with red and green circles, respectively.

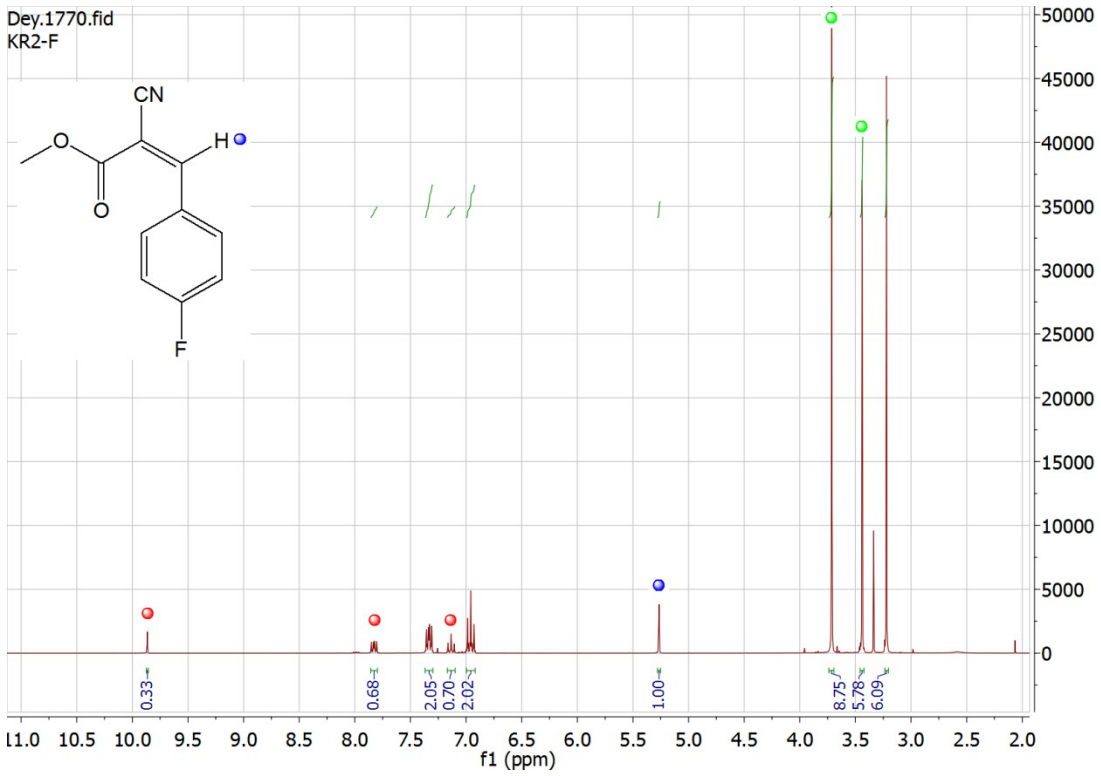

Fig. S46 ^{1}H NMR spectrum of as synthesized 2-cyano-3-(4-fluorophenyl)methylacrylate in $CDCl_3$. Signals for unreacted aldehyde and methylcyanoacetate are represented with red and green circles, respectively.

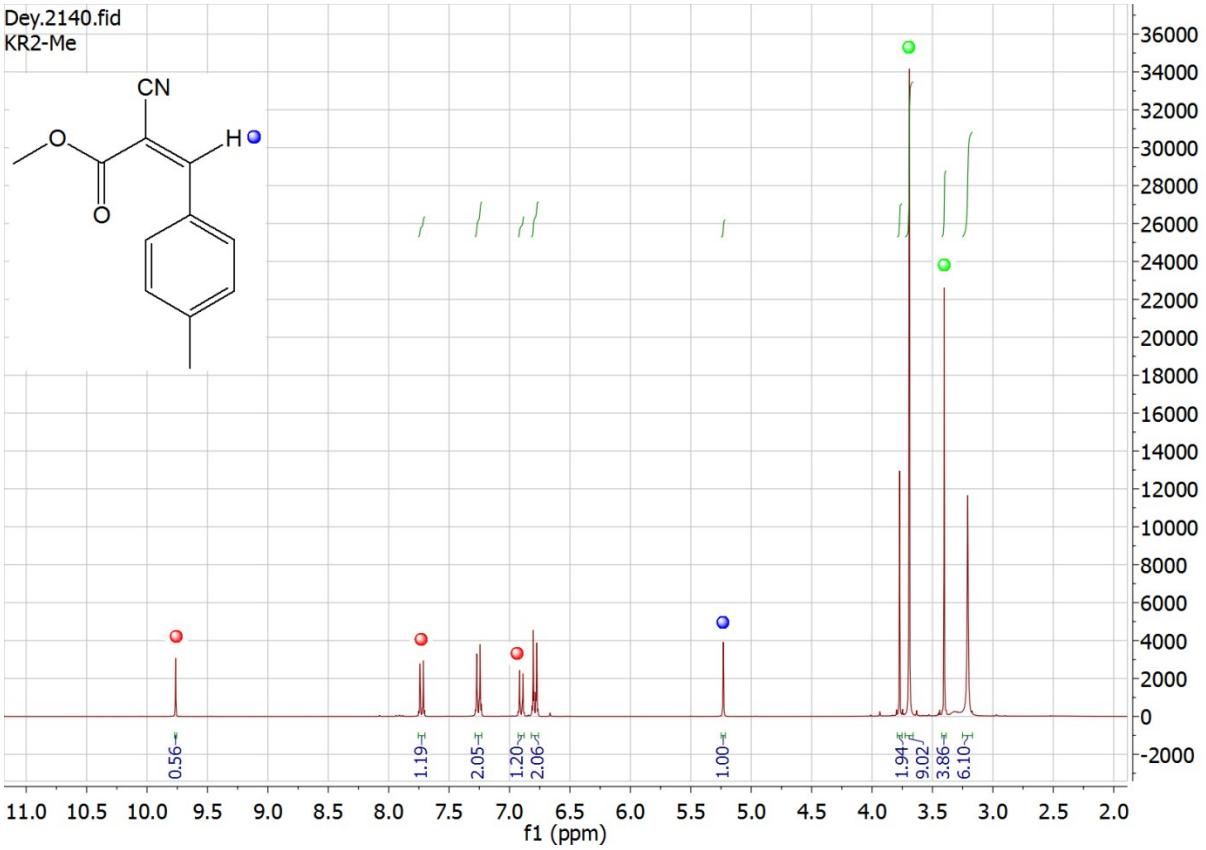

Fig. S47 ^{1}H NMR spectrum of as synthesized 2-cyano-3-(4-tolyl)methylacrylate in $CDCl_3$. Signals for unreacted aldehyde and methylcyanoacetate are represented with red and green circles, respectively.

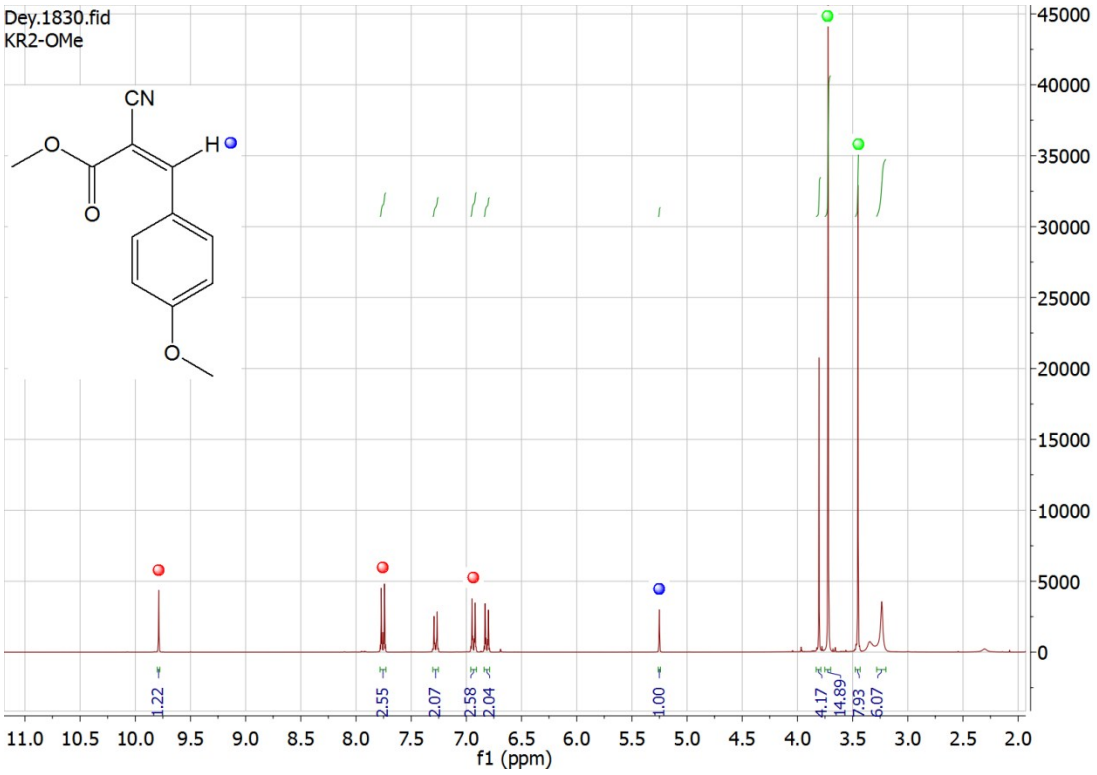

Fig. S48 ^{1}H NMR spectrum of as synthesized 2-cyano-3-(4-methoxyphenyl)methylacrylate in $CDCl_3$. Signals for unreacted aldehyde and methylcyanoacetate are represented with red and green circles, respectively.

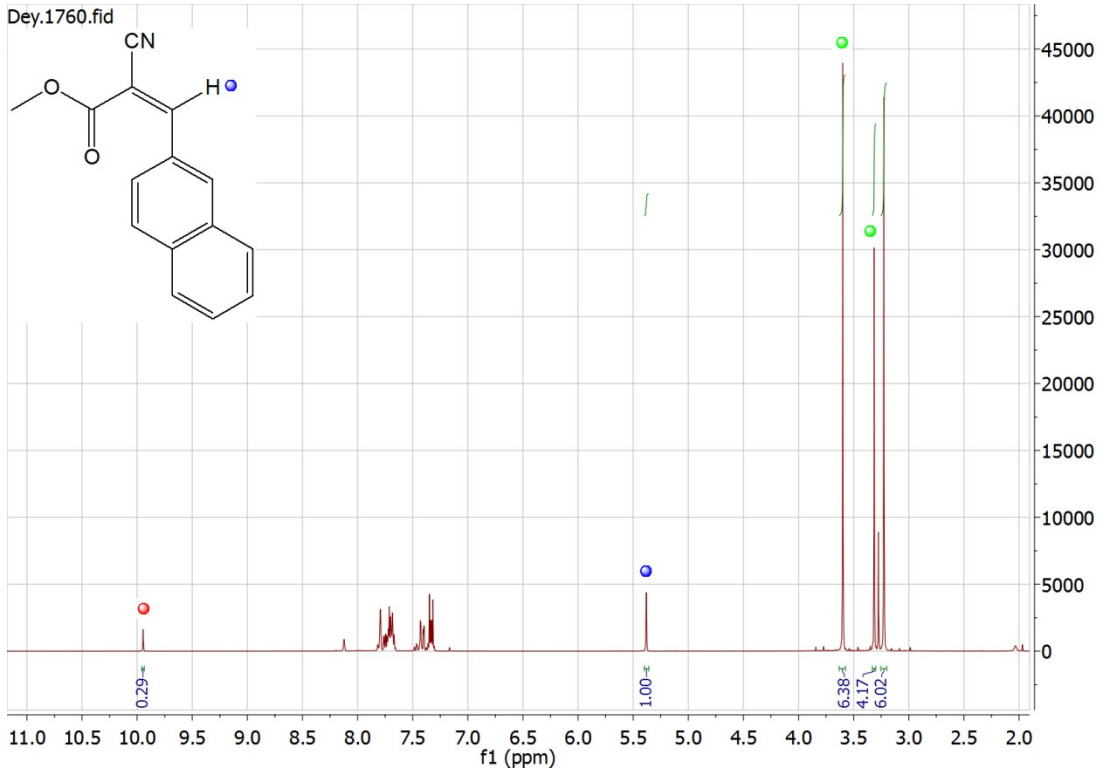

Fig. S49 ^{1}H NMR spectrum of as synthesized 2-cyano-3-(naphthyl)methylacrylate in $CDCl_3$. Signals for unreacted aldehyde and methylcyanoacetate are represented with red and green circles, respectively.

11. Characterization of the Henry reaction products.

Table S3: Catalytic data of the activated MPU catalysed Henry reaction.

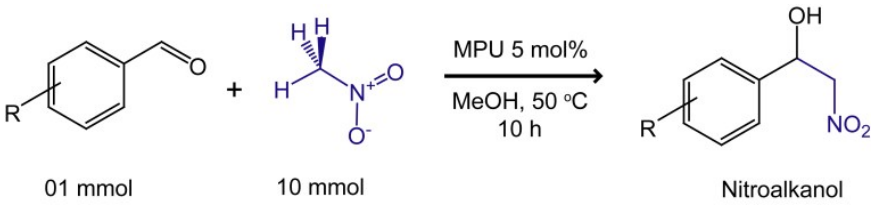

01 mmol 10 mmol Nitroalkanol

Entry	Aromatic aldehydes	Yield (%)[a] of β-nitroalkanol	
		Run-1	Run-2
1	Benzaldehyde	00	00
2	4-Nitrobenzaldehyde	94	95
3	3-Nitrobenzaldehyde	93	97
4	2-Nitrobenzaldehyde	96	93
5	4-Carboxybenzaldehyde	91	90
6	4-cyanobenzaldehyde	95	99
7	4-Chlorobenzaldehyde	77	75
8	4-Methylbenzaldehyde	20	22
9	4-Methoxybenzaldehyde	00	00
10	2-Naphthaldehyde	00	00
11	9-anthracenealdehyde	00	00
12	Biphenyl-4-carboxaldehyde	00	00

[a] yields are calculated with respect to the unreacted aldehydes present in the reaction mixture (see the ^{1}H NMR spectral analysis, Fig S42-S49)

[b] TON (Turnover number) = Moles of desired product formed/moles of catalyst used.

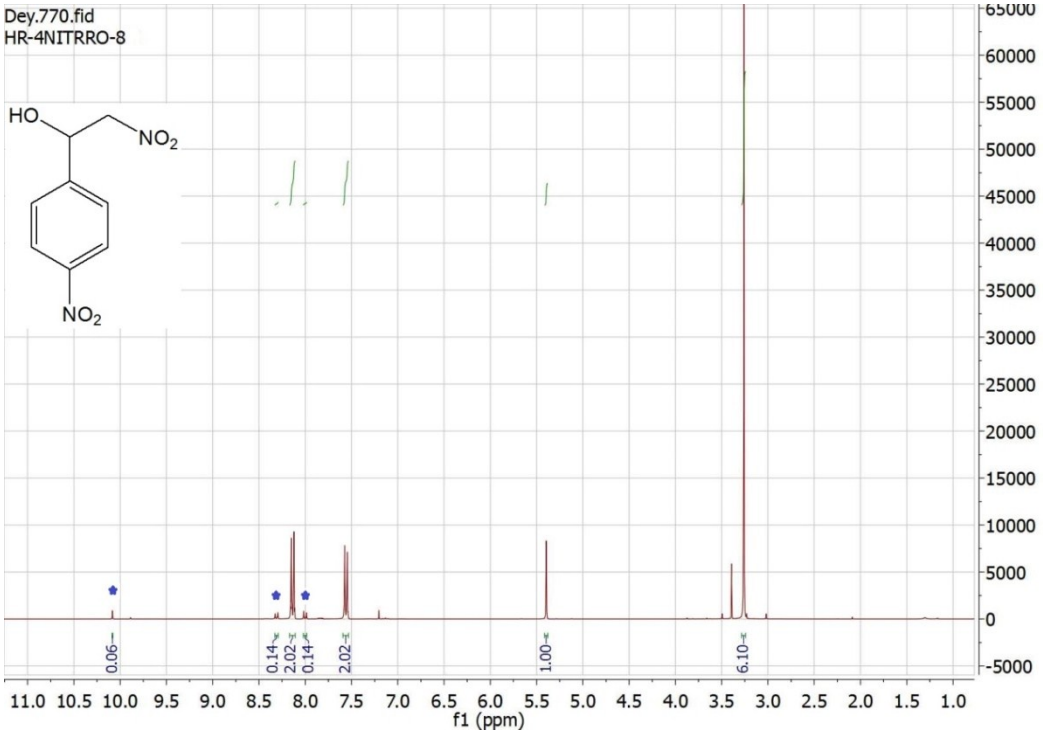

Fig. S50 ^{1}H NMR spectrum of as synthesized 2-nitro-1-(2-nitrophenyl)ethanol in $CDCl_3$. Signals for unreacted aldehyde are represented with blue stars.

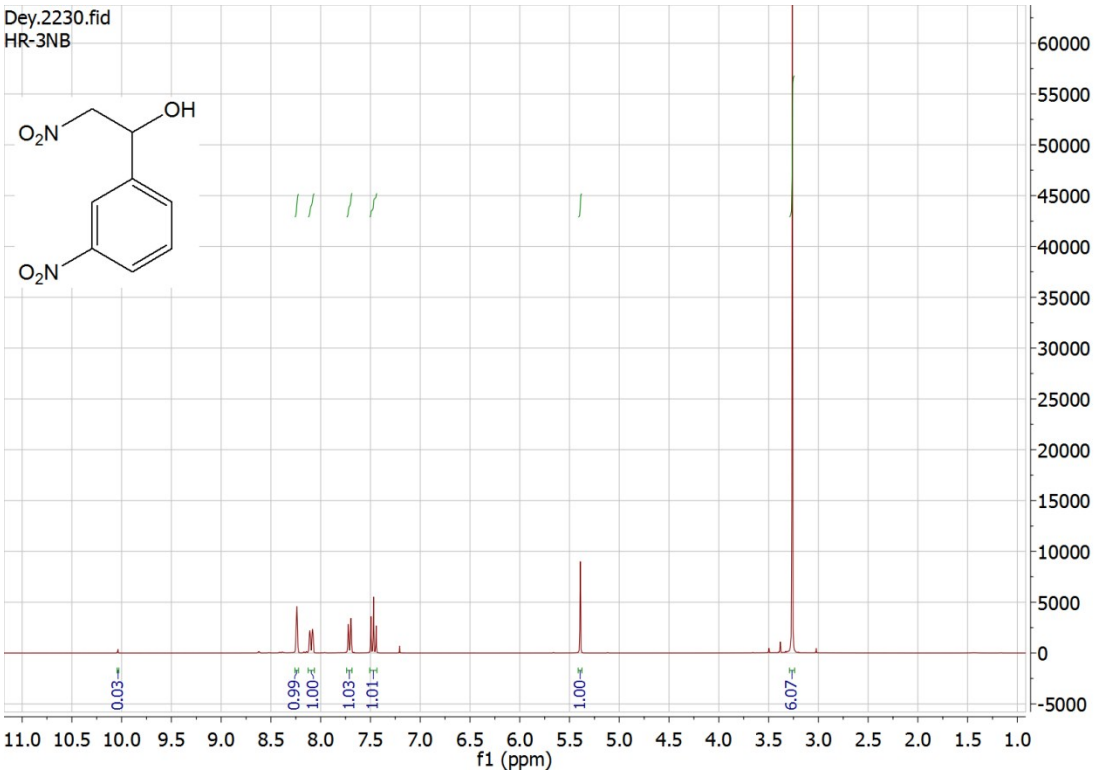

Fig. S51 ^{1}H NMR spectrum of as synthesized 2-nitro-1-(3-nitrophenyl)ethanol in $CDCl_3$.

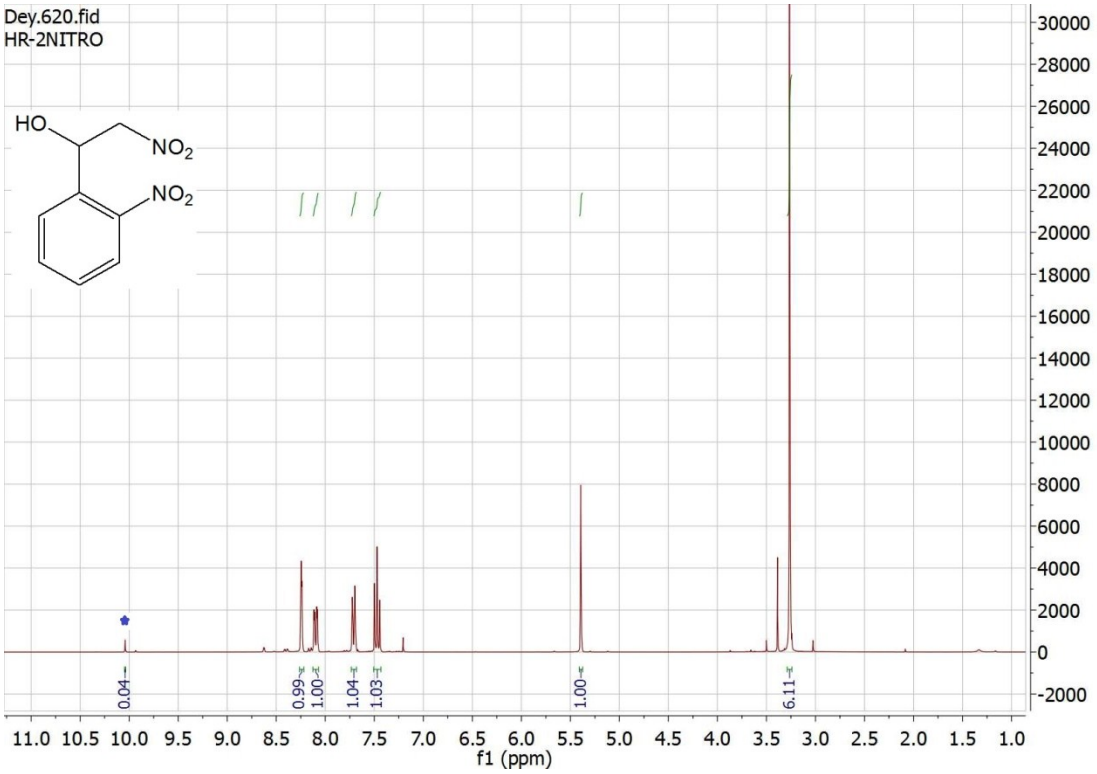

Fig. S52 ^{1}H NMR spectrum of as synthesized 2-nitro-1-(4-nitrophenyl)ethanol in $CDCl_3$. Signals for unreacted aldehyde are represented with blue stars.

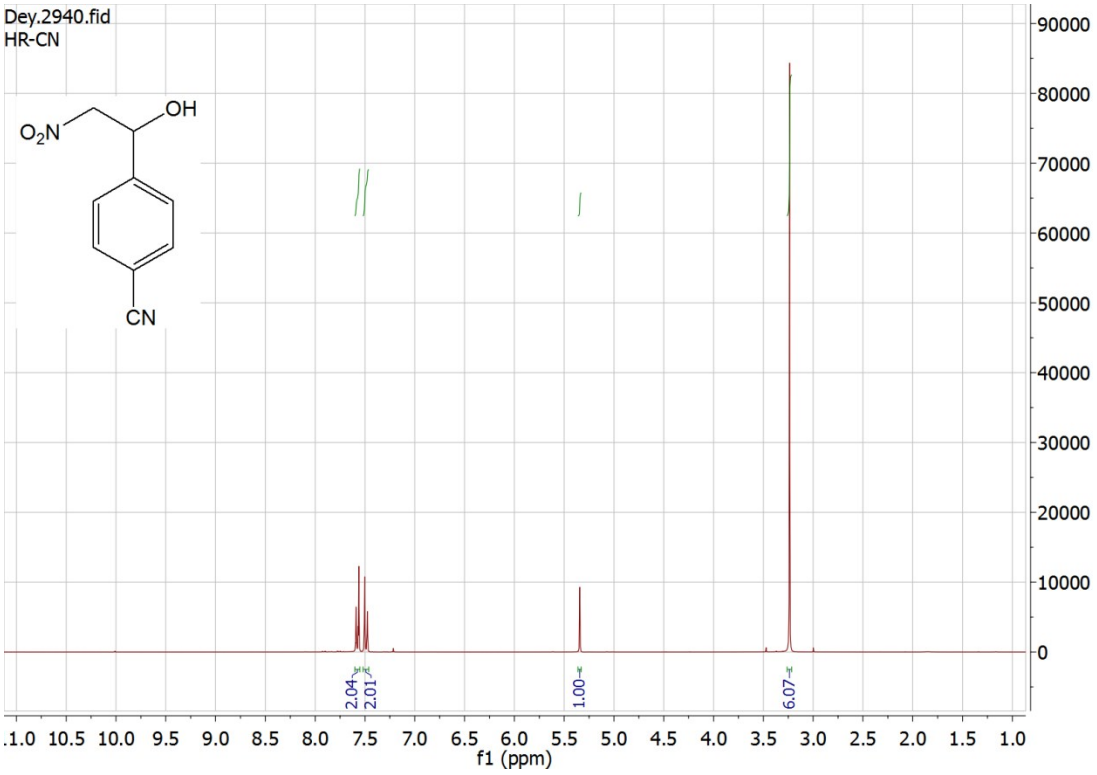

Fig. S53 ^{1}H NMR spectrum of as synthesized 2-nitro-1-(4-cyanophenyl)ethanol in $CDCl_3$.

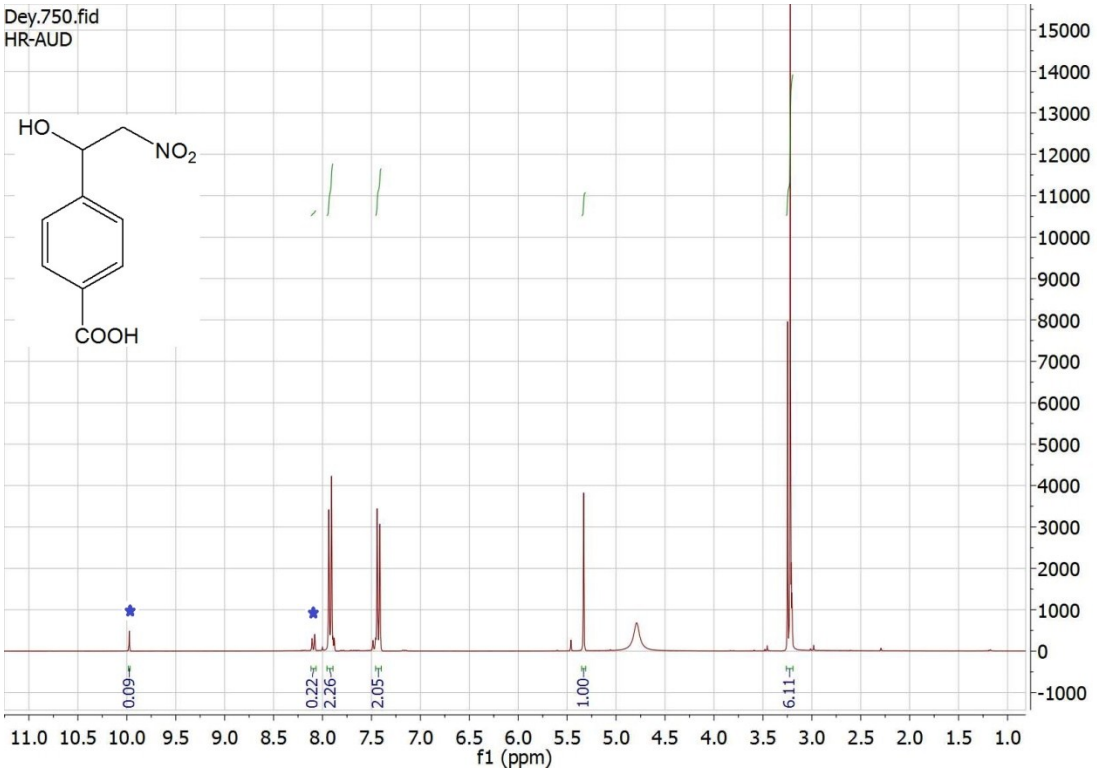

Fig. S54 ^{1}H NMR spectrum of as synthesized 2-nitro-1-(4-carboxyphenyl)ethanol in $CDCl_3$. Signals for unreacted aldehyde are represented with blue stars.

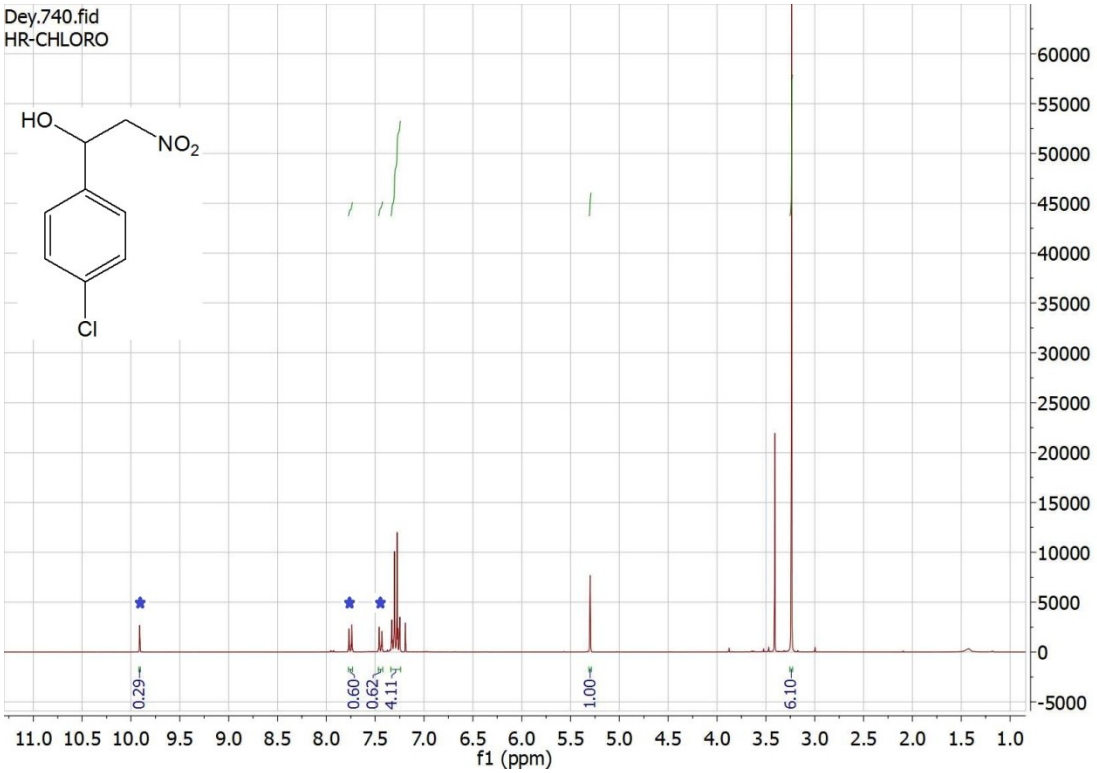

Fig. S55 ^{1}H NMR spectrum of 2-nitro-1-(4-chlorophenyl)ethanol in $CDCl_3$. Signals for unreacted aldehyde are represented with blue stars.

12. Homogeneous base catalysed Knoevenagel reaction in THF.

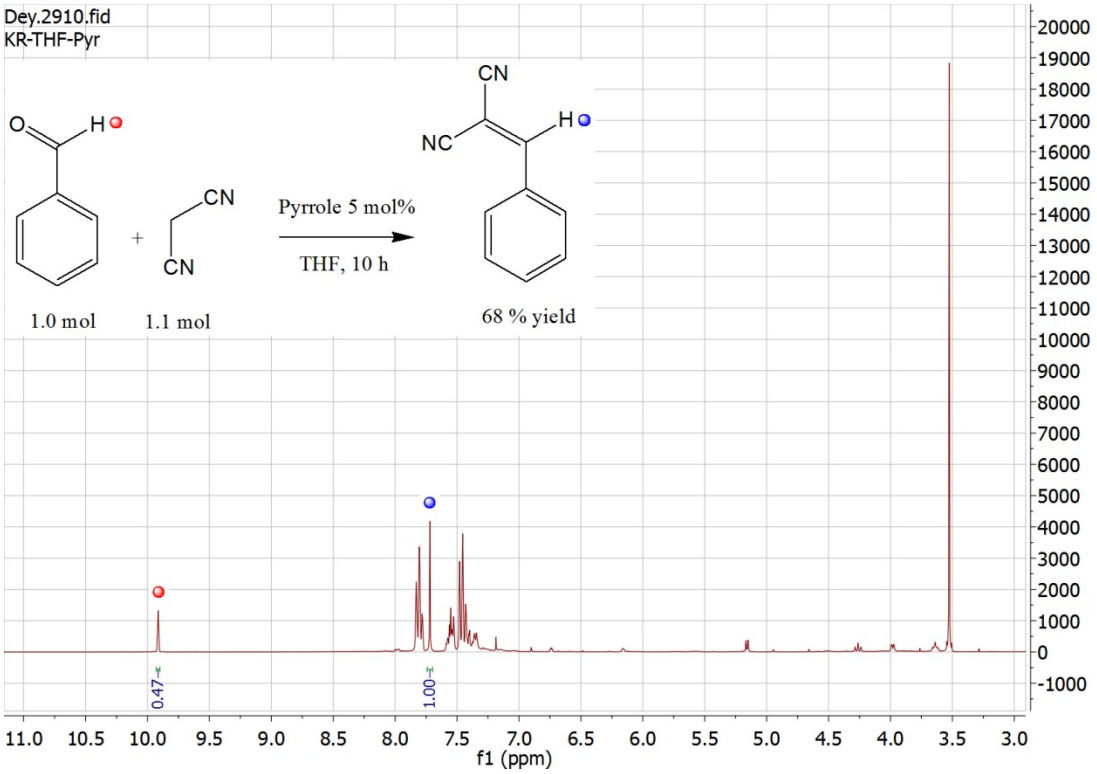

Fig. S56 ^{1}H NMR spectrum of pyrrole (5 mol%) catalysed Knoevenagel reaction in THF.

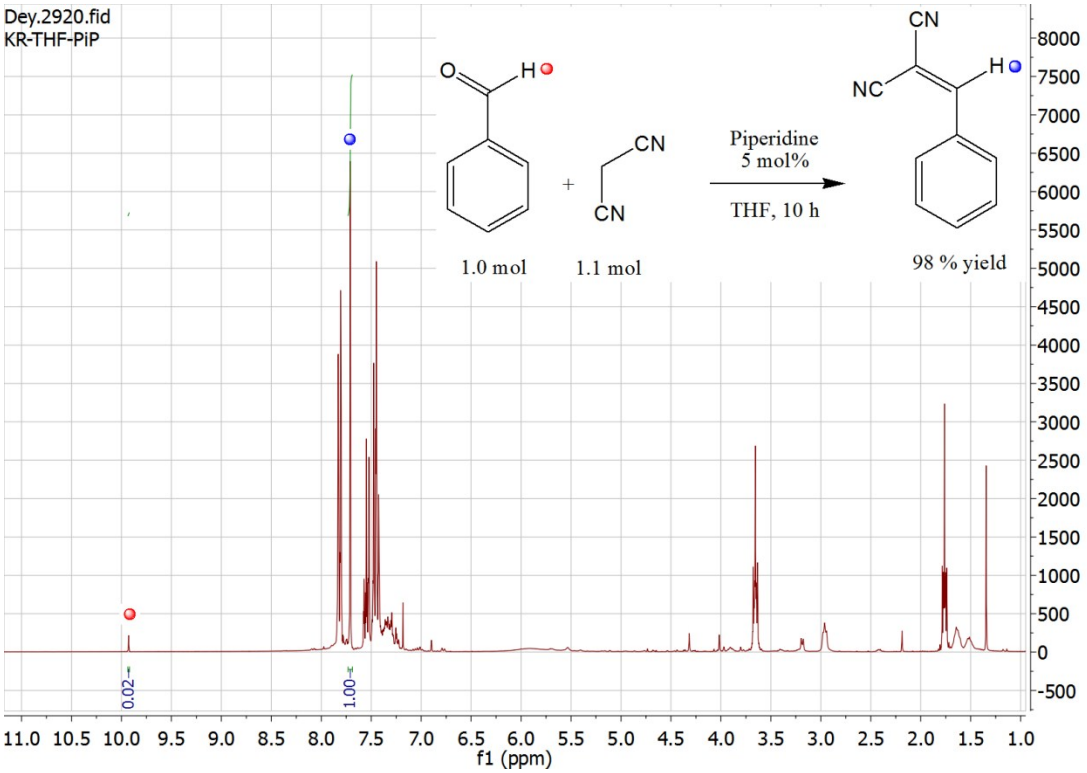

Fig. S57 ^{1}H NMR spectrum of piperidine (5 mol%) catalysed Knoevenagel reaction in THF.

Table S4: Catalytic data of the activated MPU catalysed Knoevenagel reaction of methylcyanoacetate with various aromatic aldehydes in methanol at 50 °C for 10 h.

1.0 mmol 1.1 mmol Conjugated Enone

entry	Aromatic aldehydes	5 mol% MPU	Without MPU
1	benzaldehyde	93	28
2	4-chlorobenzaldehyde	90	09
3	4-fluorobenzaldehyde	82	26
4	4-tolualdehyde	89	20
5	4-anisaldehyde	66	00
6	2-naphthalenealdehyde	82	05
7	9-anthracenealdehyde	00	00
8	biphenyl-4-carboxaldehyde	00	00
9	2-nitrobenzaldehyde	90	12
10	4-nitrobenzaldehyde	97	95